

Assessment of 69 kV Underground Cable Thermal Ratings
using Distributed Temperature Sensing

by

Travis Stowers

A Thesis Presented in Partial Fulfillment
of the Requirements for the Degree
Master of Science

Approved November 2015 by the
Graduate Supervisory Committee:

Daniel Tylavsky, Chair
George Karady
Keith Holbert

ARIZONA STATE UNIVERSITY

December 2015

ABSTRACT

Underground transmission cables in power systems are less likely to experience electrical faults, however, resulting outage times are much greater in the event that a failure does occur. Unlike overhead lines, underground cables are not self-healing from flashover events. The faulted section must be located and repaired before the line can be put back into service. Since this will often require excavation of the underground duct bank, the procedure to repair the faulted section is both costly and time consuming. These added complications are the prime motivators for developing accurate and reliable ratings for underground cable circuits.

This work will review the methods by which power ratings, or *ampacity*, for underground cables are determined and then evaluate those ratings by making comparison with measured data taken from an underground 69 kV cable, which is part of the Salt River Project (SRP) power subtransmission system. The process of acquiring, installing, and commissioning the temperature monitoring system is covered in detail as well. The collected data are also used to evaluate typical assumptions made when determining underground cable ratings such as cable hot-spot location and ambient temperatures.

Analysis results show that the commonly made assumption that the deepest portion of an underground power cable installation will be the hot-spot location does not always hold true. It is shown that distributed cable temperature measurements can be used to locate the proper line segment to be used for cable ampacity calculations.

ACKNOWLEDGMENTS

I would like to thank my advisor Dr. Daniel Tylavsky for making this research opportunity available and for his guidance and support throughout my graduate studies at Arizona State University.

I would also like to express my appreciation to Salt River Project for providing the necessary resources to complete this work. The support of Jim Hunt, Catherine Obrien and Bryce Priest of the Electrical Engineering Services department at SRP was invaluable throughout the course of my research. The contributions of Brady Dressendorfer and Nathan Cowan were also crucial to the completion of the physical installation work at the data collection site. I would also like to extend thanks to Mike Unser and Joe Pacheco of SRP's communications department for their assistance in making the necessary fiber optic splicing required throughout the course of the project.

Finally, I would like to express my sincere gratitude to Dr. George Karady and Dr. Keith Holbert for their time and consideration as members of my graduate supervisory committee.

TABLE OF CONTENTS

	Page
LIST OF TABLES	vi
LIST OF FIGURES	vii
NOMENCLATURE	x
CHAPTER	
1. INTRODUCTION.....	1
1.1 Background	1
1.2 Motivation:.....	2
1.3 Research Goal and Project Scope.....	3
2. LITERATURE REVIEW	4
2.1 Underground Power Transmission Cable Components	4
2.2 Underground Cable Installations.....	8
2.3 Cable Ampacity Calculation	9
2.4 Cymcap.....	11
2.5 Distributed Temperature Sensing (DTS).....	14
3. SELECTION OF MONITORED UNDERGROUND (UG) LINE.....	19
4. BRANDOW – PICKRELL EXISTING INSTALLATION	20
4.1 Overview	20

CHAPTER	Page
4.2 Duct Bank Configurations and Materials.....	22
4.3 Section Requiring Structural Reinforcement	26
4.4 Existing (assumed) Hot Spot Location and Cable Ampacity.....	27
5. DTS LABORATORY TESTING.....	29
5.1 Laboratory Test Setup	30
5.2 Laboratory Test Results	32
6. DTS INSTALLATION.....	34
6.1 NEMA Rated Outdoor Enclosure	35
6.2 AC Power Connection.....	36
6.3 Fiber-Optic Cable Installation, Identification, and Splicing	37
7. EXPERIMENTAL SETUP	39
7.1 Measured Cable/Phase and Fiber Connection.....	39
7.2 Length of Underground Cable.....	40
8. DTS COMMISSIONING AND PRELIMINARY RESULTS.....	42
8.1 DTS Commissioning and Charon3 Software.....	42
8.2 Data Collection.....	46
8.3 Preliminary DTS Results.....	47
9. MEASURED RESULTS AND ANALYSIS	52

CHAPTER	Page
9.1 Hot-Spot Locating	52
9.2 Measured Temperature at Hot-Spot Location	55
9.3 Evaluation of Steady-State Ampacity at Hot-Spot Location	56
9.4 Comparison of Cymcap Transient Results to Measured DTS Data.....	58
9.5 Adjustment of Ambient Temperature	64
9.6 Re-Evaluation of Steady-State Ampacity with Adjusted Ambient Temperature	67
10. SUMMARY, CONCLUSIONS AND FUTURE WORK	68
10.1 Distributed Temperature Sensing (DTS)	68
10.2 Hot-Spot Locating	68
10.3 Ampacity Calculation at new Hot-Spot Location.....	70
10.4 Ambient Temperature Adjustment	70
10.5 Reevaluation of Steady-State Ampacity at Hot-Spot Location	71
10.6 Proposed Future Work.....	71
REFERENCES	73

LIST OF TABLES

Table	Page
5.1: Test Setup Results.....	32
8.1: DTS Measurement Parameters	46
9.1: Cymcap Model Input Data.....	57
9.2: Cymcap Transient Analysis Parameters	60
9.3: Cymcap Transient Analysis Results and Required Ambient Temperature Adjustment	66

LIST OF FIGURES

Figure	Page
2.1: Cross Section Schematic of Nexans Cable	4
2.2: Concentric Neutral Length-of-Lay	7
2.3: Vertical Duct Bank Configuration [3]	8
2.4: Thermal Equivalent Circuit	9
2.5: Cymcap Graphical Representation with Steady-State Ampacity Shown	13
2.6: Cymcap Transient Temperature and Load Shape	14
2.7: DTS Operation	16
2.8: DTS Dual Channel Measurement	17
4.1: Overhead View of Brandow to Pickrell Underground Line	20
4.2: Riser Pole 30 Fiber Splice Box	21
4.3: UG Duct Bank Profile - Section A	22
4.4: UG Duct Bank Profile - Section B	23
4.5: Horizontal Configuration [3]	24
4.6: Section at Manhole and Riser Poles [3]	24
4.7: Vertical Configuration [3]	25
4.8: Duct Bank at Reinforced Section [3]	26
4.9: APS 230kV UG Line Crossing With Brandow - Pickrell Line	27
5.1: Test Setup Simulating Brandow – Pickrell Fiber Optic Arrangement	30
5.2: Test Setup With Coiled Reference Temperature Sections	31
5.3: DTS OTDR Showing Boundaries for Each Fiber Section	31
5.4: Section B DTS Trace - Reference Temperature at 31.1°C	32

Figure	Page
6.1: DTS Enclosure Installed Next to Riser Pole 24.....	34
6.2: NEMA Rated Outdoor Enclosure for DTS System.....	35
6.3: Conduit Trench for AC Power Cable to DTS.....	36
6.4: Length Markings on Corning Fibers.....	38
6.5: Diagram Showing the Label Associated with Each UG Cable	38
7.1: Brandow-Pickrell Fiber Optic Configuration	39
7.2: Brandow-Pickrell UG Cable SA Path.....	40
8.1: Charon3 Quick Start Length Scan of Optical Channels 1 and 2	42
8.2: Backscatter Scan of Fiber SA	44
8.3: Temperature vs Distance for Complete SA Loop.....	45
8.4: DTS Measurement Parameters for Cable SA	45
8.5: Measured Temperature of Corning Optical Fiber 26 meter from DTS	48
8.6: DTS Backscatter Data Showing Fiber Splice Locations	49
8.7: DTS Temperature Trace Aligned With SRP UG Profile Map	51
9.1: Hot-Spot Occurrences between 35 and 565 Meters.....	52
9.2: Hot-Spot Location plot Matched to UG Profile.....	53
9.3: Hot-Spot Location Plot - Cropped between 1100 and 1200 Feet on UG Profile	53
9.4: DTS Temperature Trace Aligned with UG Profile - Hot-Spot Location Identified..	54
9.5: Raw DTS Temperature Data at the Hot-Spot Location.....	55
9.6: DTS Daily Average Temperature at the Hot-Spot Location	55
9.7: Cymcap Duct Bank Model at Hot-Spot Location.....	56
9.8: Smoothed DTS Temperature Data and Line Loading	60

Figure	Page
9.9: Cymcap Load Shape and Predicted Temperature	61
9.10: Measured DTS and Predicted Cymcap Temperatures with Cymcap Ambient Temperature at 35C.....	62
9.11: Measured DTS and Adjusted Cymcap Temperatures.....	63
9.12: Asphalt Temperature above Hot-Spot Location	65
9.13: Cymcap Reevaluated Steady-State Ampacity	67

NOMENCLATURE

$a[\frac{W}{m^2C}]$	Convection Coefficient
$D[m]$	Diameter of UG cable to center of embedded fiber optic cable
$\Delta t[C]$	Temperature difference between ambient and conductor
K	Temperature, Kelvin
$l [m]$	Length-of-Lay
$L[m]$	Length of underground cable
$L_e[m]$	Distance from Earth Surface to Closest Cable
$L_f[m]$	Length of embedded fiber optic cable
$r_0[\frac{C \cdot m}{W}]$	Thermal Resistivity of Native Soil
$R_d[\frac{C \cdot m}{W}]$	Thermal resistance of the cable dielectric insulation
$R_e[\frac{C \cdot m}{W}]$	Equivalent thermal resistance of earth/backfill materials
$R_s[\frac{C \cdot m}{W}]$	Thermal resistance of the cable screen
sf	Unitless factor used to scale the embedded fibers of the Nexans UG power cables
T_{avg}	Average Temperature
$t_{amb}[C]$	Ambient temperature

$t_c[\text{C}]$	Cable conductor temperature
$W_c[\frac{\text{W}}{\text{m}}]$	Heat generated by the cable conductor
$W_d[\frac{\text{W}}{\text{m}}]$	Heat generated by the cable dielectric insulation
$W_s[\frac{\text{W}}{\text{m}}]$	Heat generated by the cable screen

1. INTRODUCTION

1.1 Background

Growing urbanization and increased emphasis on aesthetics are just two of the major drivers for installing underground power transmission and distribution circuits. Underground cables provide increased system reliability due to their reduced exposure to environmental strains but their design and construction offer greater difficulties than those of traditional overhead lines.

The major disadvantages associated with using underground power cables are the added cost of installation, increased environmental disruption and increased repair time due to underground cable failure. While underground cables are more reliable than overhead, fault locating and repair can be much more difficult and costly than that of an overhead system. The most easily controlled cause of underground cable failure is excess heating of the cable insulation. The power capacity of an underground cable is limited by the maximum allowable operating temperature of the cable insulation. Overhead lines are insulated and cooled by open air and self-heal from arc flashovers. Conversely, the dielectric insulating materials used in underground cables are susceptible to degradation caused by heating and do not self-recover when flashover occurs.

Cable heating is a direct function of the power carried by an underground cable and therefore a limiting steady-state current rating (ampacity) is used to rate the amount of electrical current allowed to flow through the line. Cable ampacity is defined as the amount of electrical current that can flow in an underground cable which results in the maximum allowable operating temperature of the cable conductor.

1.2 Motivation:

Underground cable installations are typically operated well below their steady state ratings. These ratings however, are calculated assuming a “worst-case” scenario which means that the ampacity is overly conservative for all but the hottest days of the year. Ambient temperature and burial depth are the two main factors that control the rate of heat flow away from the cable circuit. For most underground cable installations the maximum expected ambient temperature and the deepest portion of the line are used for ampacity calculations. While this serves to protect the cables from overheating, it also causes the cables to be significantly underutilized throughout a majority of their functional life.

Another concern with the above rating approach is that the hot-spot of an installed underground cable may not necessarily be at its deepest portion, which is the usual assumption used when performing temperature calculations. This source of error in ampacity calculations may or may not be conservative. The hot-spot of an underground cable installation is defined as the section of cable that experiences the highest temperature at a given loading relative to the entire cable length. Since the hot-spot section will reach critical temperature first, it is used as the limiting portion for the underground installation. However, crossings with other underground cables, water and gas lines and other complexities in the underground environment can make determining the system hot spot more complex. Additionally, underground cables in the vicinity of high solar irradiance, such as those located inside riser poles or close to asphalt paving, could potentially experience higher heating than the traditional hot spot location due to the influence of the solar heat flux.

The much higher cost of installation and repair for underground transmission lines makes it especially important to properly select the correct location and geometry used in calculating cable ampacities. Also, more accurate thermal models can allow for more accurate steady-state ratings and potentially the development of dynamic ratings. Both of these can potentially increase the utilization of both existing and new underground installations.

1.3 Research Goal and Project Scope

The Salt River Project (SRP) power and water utility company currently operates sixteen 69 kV underground transmission lines. The ampacities for each installation were originally calculated using traditional closed form mathematical formulae and later updated with more sophisticated iterative computer based methods, using *Cymcap*. The intention of this research is to collect real-time temperature data from one of SRP's underground 69 kV transmission lines using advanced Distributed Temperature Sensing (DTS) equipment and to evaluate the accuracy of these existing ratings. Also checked will be the assumptions made when performing ampacity calculations, such as hot spot location, ambient temperature and soil/backfill thermal properties. More accurate cable ratings have the potential to offer improved system reliability and expanded system capacity by fully utilizing the potential of installed underground systems.

2. LITERATURE REVIEW

2.1 Underground Power Transmission Cable Components

Underground transmission lines are required to operate at high voltage while being in close proximity to grounded materials. This creates a challenge because the cable needs to be both protected from physical damage and electrically insulated with consideration being given to the heat generated during cable operation. Operating voltages and currents as well as environmental considerations dictate the ultimate cable construction that should be selected for a given installation. The geometry and materials used in an underground cable both affect the ultimate temperature and thus the cable's rating. The analyses carried out in this thesis will involve only 1500MCM XLPE underground cables.

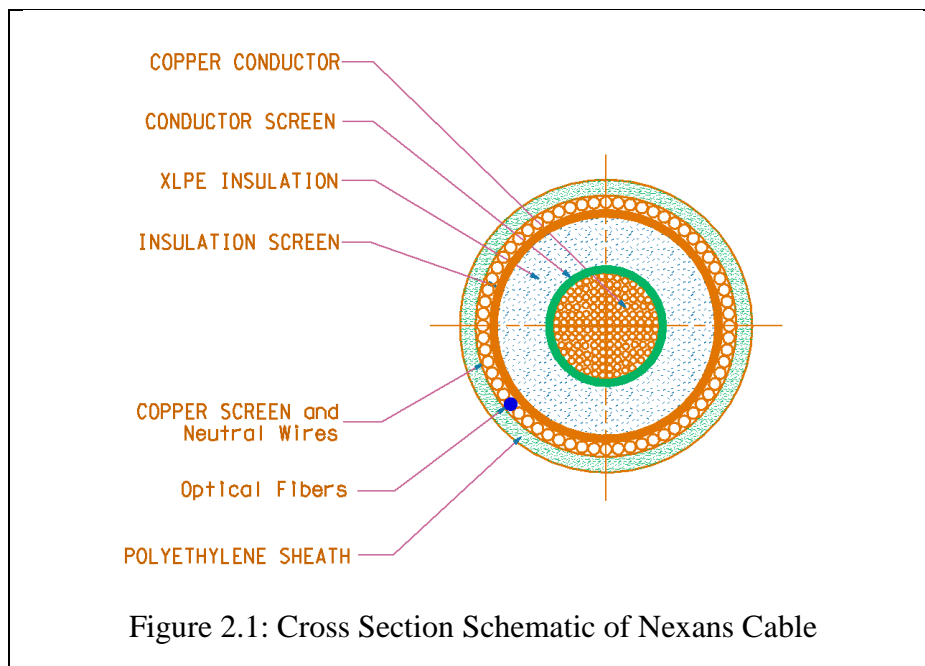


Figure 2.1 shows a cross-sectional schematic view of one of the 69kV underground power cables monitored in this research. The individual cable components of Figure 2.1 are described below.

2.1.1. Cable Conductor:

Cable conductors are made of either copper or aluminum and with varying geometry [1]. Conductor cross-section geometries include stranded, round, quarter segment, hollow core, six-segment, oval and others. Both the conductor material and construction affect the amount of heat generated by the cable. The conductor shown in Figure 2.1 is a 1500MCM (thousand circular mills) copper core with a compact stranded design.

2.1.2. Conductor Screen

The conductor screen is layered between the conductor and the insulation material [2]. Along with adding strength to the cable, the main function of the conductor screen is to help create a uniform, radial electric field distribution around the conductor. This helps to reduce the stresses imposed on the cable insulation.

2.1.3. Insulation

High-density cross-linked polyethylene (XLPE) is the material of choice for most high voltage underground cables for both its electrical as well as thermal characteristics. XLPE is rated for a continuous conductor current of 90°C and emergency ratings of up to 140°C [2].

2.1.4. Insulation Screen

The insulation screen provides a uniform electric field distribution, relieves surge voltage by providing uniform cable capacitance and provides a low impedance path for line charging current [2].

2.1.5. Cable Screen and Concentric Neutral Wires

The primary purpose of the cable screen, which is made of copper, is to ensure that there is no electric field outside the cable [2]. It also provides radial waterproofing for the cable insulation as well as active conductors for carrying of capacitive charging currents and zero sequence short circuit currents. The screen also provides physical strength for the cable construction. Some cable manufacturers may include fiber sensing cables in the position of one of the neutral conductors (see Figure 2.1). The Nexans cable under study in this paper includes 6 optical fibers contained in one stainless steel tube in the screen and neutral wire layer.

The concentric neutral wires may travel parallel to the conductor in a simple straight path or may be wound around the cable in a helical fashion. For neutral wires that are wound, the linear distance along the cable for one complete turn is known as the length-of-lay of the cable. Figure 2.2 shows the path of the concentric neutral wires and fiber optic cable for the Nexans cable of Figure 2.1. The length-of-lay for the Nexans UG cable is 400 mm for each complete turn of the neutral wires or optical fiber. Using the diameter (D), as measured from the cable screen layer and the length of lay (l) the ratio of fiber length (L_f) to cable length (L) can be calculated.

$$\frac{L_f}{L} = \frac{\sqrt{l^2 + \pi^2 D^2}}{l} = 1.163[\text{unitless}] \quad (2.1)$$

From (2.1) we can see that for an arbitrary meter of cable the concentric neutral wires and optical fibers will measure 1.163 meters.

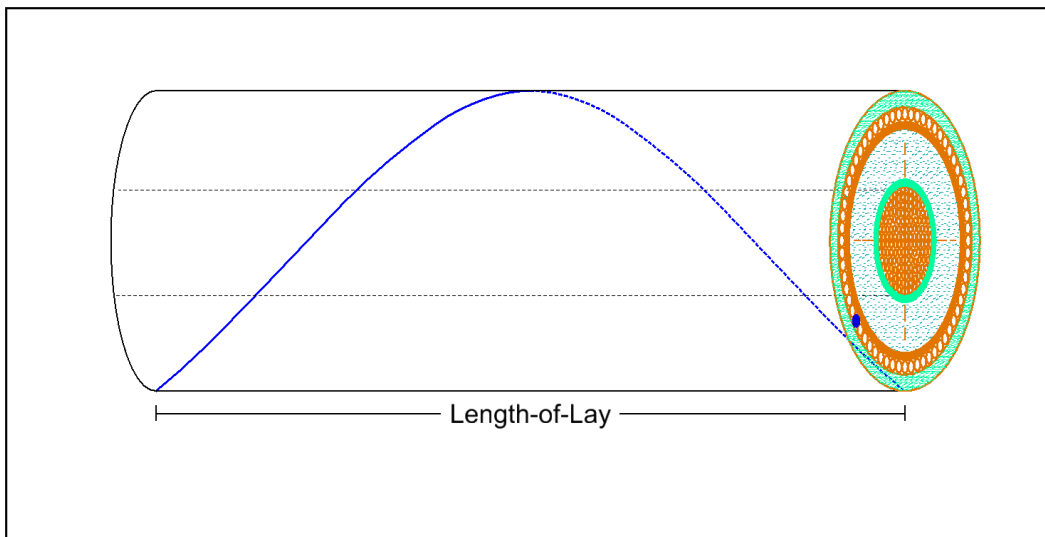


Figure 2.2: Concentric Neutral Length-of-Lay

2.1.6. Sheath

The cable sheath is the final layer and the first line of defense for protecting the cable from physical damage. Cable jacket materials include polyethylene (PE), propylene rubber and PVC. The Nexans cable shown in Figure 2.1 has a PE sheath.

2.2 Underground Cable Installations

The surrounding environment for underground cable installations is as important to determining cable temperature as the cable construction itself. Factors such as burial depth, conductor spacing and geometry all contribute to how quickly heat is able to flow outward from the conductor. Underground cables used for transmission are typically enclosed in PVC conduit that has been encased inside a concrete duct bank. The duct bank is then covered with a backfill material which is more stable than the native soil and has desirable and known thermal characteristics. The thermal properties of each of the materials used in every layer must be known by direct measurement or by calculation in order to accurately determine cable ampacity. Figure 2.3 shows an example design for a vertical configuration duct bank installation.

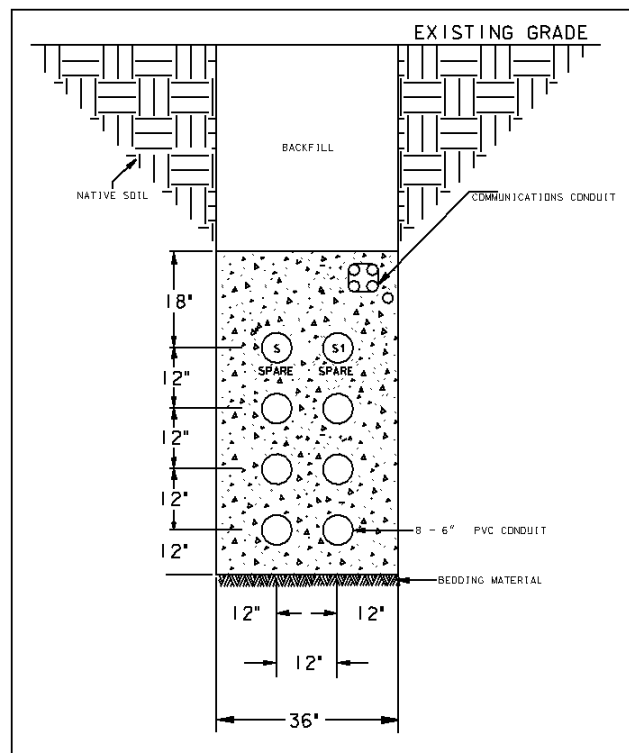


Figure 2.3: Vertical Duct Bank Configuration [3]

2.3 Cable Ampacity Calculation

Given a particular operating voltage and installation environment, cable ampacity is determined by the maximum conductor current that does not create conductor temperatures that exceed those allowed by the cable insulating materials. Ampacity calculation is largely based on the 1957 Neher and McGrath method [4] which describes methods for both steady-state and transient temperature calculation.

The heat generated by the cable is radiated outward through the various cable components described in section 2.1, through the cable conduit and duct bank, and ultimately to the earth surface and to open air. To determine temperature drop across each element it is useful to recognize that the system is analogous to an electrical circuit with heat flow analogous to electrical current and temperature drop analogous to voltage drop across the thermal resistances. Figure 2.4 shows an example of a thermal electrical equivalent circuit where the current sources represent the heat sources of the cable's conductor, dielectric insulating material and metallic screen and the resistances represent the thermal resistances of the cable layers and surrounding environment.

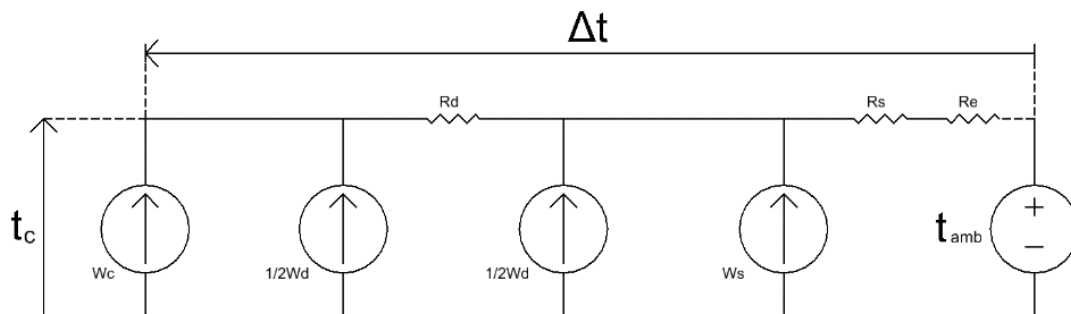


Figure 2.4: Thermal Equivalent Circuit

The term Δt in Figure 2.4 represents the temperature difference between the ambient and cable conductor and is a function of conductor current and the surrounding thermal resistances. Since the thermal resistances and ambient temperature are assumed to be constant, Δt can be found as a function of only conductor current. The thermal resistances (R_d , R_s and R_e) of Figure 2.4 are determined by the material properties of the surrounding environment and have units of $^{\circ}\text{CmW}^{-1}$.

The dielectric loss (W_d) is a function of cable capacitance(C), operating voltage (V), angular frequency (ω) and the cable loss angle (δ). The calculation of the loss angle is too lengthy to be detailed here. The curious reader can find more detailed analysis in many published works on the subject including reference source [5].

$$W_d = \omega CV^2 \tan(\delta) \text{ W m}^{-1} \quad (2.2)$$

The screen loss (W_s) is proportional to the conductor loss by the factor λ . The scaling factor λ is a function of the circulating eddy currents in the cable screen and is affected by the proximity of cables to each other and the configuration in which the screens are bonded together [6]. The calculation of the loss factor, even in advanced finite element analysis methods, is usually conducted analytically [7].

$$W_s = \lambda \cdot W_c \text{ W m}^{-1} \quad (2.3)$$

Finally, the conductor losses themselves (W_c) are a function of conductor ac resistance and current. Conductor ac resistance (R_{ac}) is a function of the cable core material and geometry, and conductor temperature.

$$W_c = R_{ac} \cdot I^2 \text{ W m}^{-1} \quad (2.4)$$

The formulation for ac resistance is shown below where α is the coefficient of variation with temperature, R_0 is the resistance at test temperature ($t=20^\circ\text{C}$) and variables γ_s and γ_p are determined by cable core geometry [6].

$$R_{ac} = R_0[1 + \alpha(t - t_0)] \cdot (1 + \gamma_s + \gamma_p) \Omega\text{m}^{-1} \quad (2.5)$$

The circuit shown in Figure 2.4 is used to derive (2.6) which gives Δt as a function the heat generated by various cable components and the surrounding thermal resistances.

$$\Delta t = \left(W_c + \frac{1}{2} W_d \right) R_d + (W_c + W_d + W_s)(R_s + R_e) \text{ C} \quad (2.6)$$

By substituting (2.3) and (2.4) into (2.6) and after some algebra, (2.7) is obtained which gives cable current as a function of temperature (ampacity).

$$I = \sqrt{\frac{\Delta t - W_d \left(\frac{1}{2} R_d + R_s + R_a + R_e \right)}{R_{ac} \cdot R_d + R_{ac} (1 + \lambda) \cdot (R_a + R_e)}} \text{ Amps} \quad (2.7)$$

The solution for ampacity described above is for steady-state operation and therefore the thermal capacitances for each thermal layer are not considered. Also, (2.7) is for a single current carrying cable. For the more complex geometries and transient results needed for analysis completed in later sections, a computer based numerical solver was employed and its operation is described below in Section 2.4.

2.4 Cymcap

Cymcap [6] is a computer program used for the calculation of power cable ampacity and temperature rise. Cymcap was developed jointly with CYME International, Ontario

Hydro and McMaster University. Temperature rise and ampacity are calculated for both steady-state and transient conditions using iterative techniques based on Neher-McGrath [4] and IEC-60287 [8] standards. CYMCAP allows the user to create graphical representations of cables, duct-banks, and back-fills. Cable loading and ambient temperature are used as input and the program iteratively solves for either steady-state ampacity or transient results of temperature versus time. Figure 2.5 shows an example underground installation created using CYMCAP. The original installation geometry used to model Figure 2.5 can be seen later in Figure 4.7.

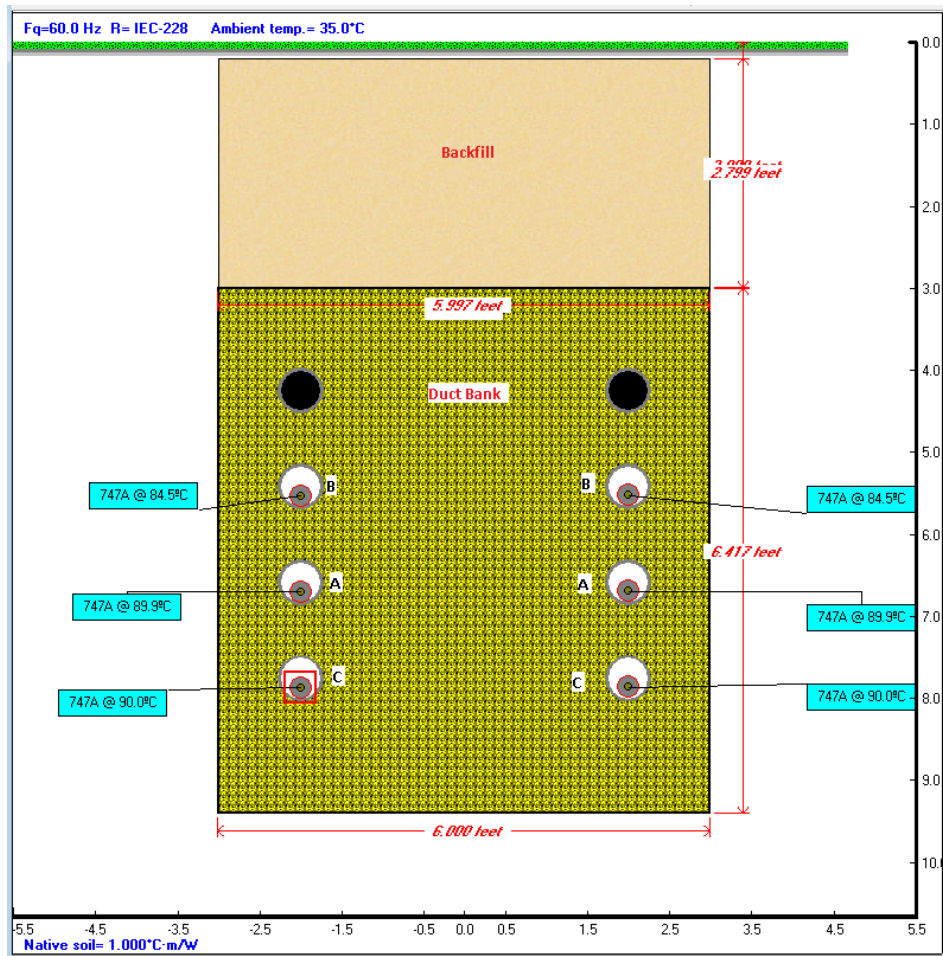


Figure 2.5: Cymcap Graphical Representation with Steady-State Ampacity Shown

Figure 2.6 shows an example of calculated cable temperature results using Cymcap and the associated input load shape.

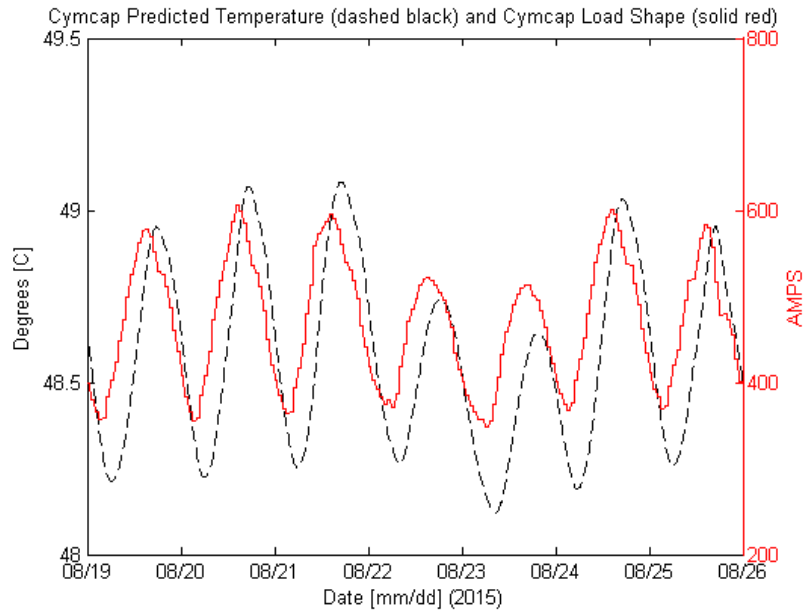


Figure 2.6: Cymcap Transient Temperature and Load Shape

2.5 Distributed Temperature Sensing (DTS)

Distributed temperature sensing is a technology that uses optical fiber cables to measure temperature using the fiber medium (typically SiO₂) itself as the temperature probe. This allows for the temperature at any point along the length of the fiber to be measured as opposed to using point sensors such as thermocouples. Of particular benefit is the fact that the optical fiber is not affected by electromagnetic interference from low frequency sources such as power cables and transformers. This makes DTS an ideal method for monitoring power system equipment which can generate high electric and magnetic fields. Using DTS a complete temperature profile of an underground line can easily be generated. With typical accuracies of around ± 1 °C, for commercial equipment, the temperature is measured at each desired point with a spatial accuracy of 1 m. Since

DTS generates an entire temperature profile of the measured cable, it is possible to directly measure, rather than infer, the hot-spot location of a cable installation.

2.5.1. DTS Theory and Operation

Distributed temperature sensing (DTS) equipment operates by analyzing the backscattered light generated when an incident monochromatic light source sent by the DTS interacts with the lattice structure of the optical fiber medium. The back scattered light is composed of three main scattered components; Rayleigh, Stokes and anti-Stokes. The Rayleigh component is due to elastic scattering and is at the same frequency as the source. The Stokes and anti-Stokes components are the result of inelastic scattering and are temperature dependent. The Stokes component is at a longer wavelength (lower frequency) and the anti-Stokes a shorter wavelength (higher frequency). The ratio of the magnitudes of Stokes and anti-Stokes backscatter component is used to determine the temperature of the fiber medium.

$$T(z, t) = \frac{\gamma}{\ln\left(\frac{P_S(z, t)}{P_{aS}(z, t)}\right) + C(t) - \int_0^z \Delta\alpha(z')dz'} \quad (2.8)$$

Equation (2.8) shows the calculation of optical fiber temperature at location z based on the ratio of the Stokes to anti-Stokes intensities [9] where:

$$\gamma(\Omega) = \frac{\hbar\Omega}{\kappa} C \quad (\Omega \text{ is the frequency shift between stokes and anti-stokes radiation})$$

$C(t)$ [unitless] is the collector sensitivity correction factor which may vary with time.

$\Delta\alpha(z)$ $\left[\frac{\text{dB}}{\text{m}}\right]$ is the differential attenuation along the optical fiber at point z [m].

$\frac{P_S(z,t)}{P_{aS}(z,t)}$ [unitless] is the measured ratio of the Stokes and anti-Stokes power reaching the DTS from measurement location z .

A simplified diagram showing single channel DTS operation can be seen in Figure 2.7.

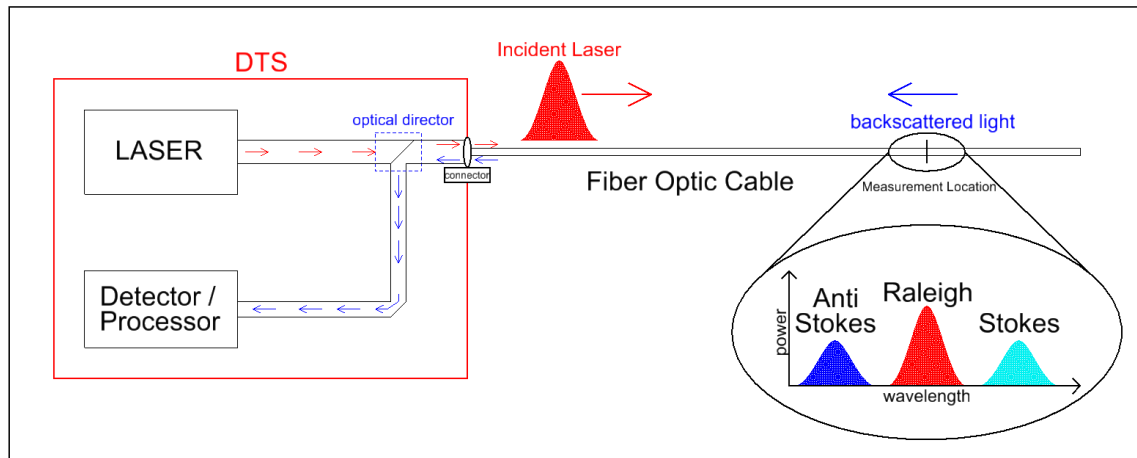


Figure 2.7: DTS Operation

2.5.2. DTS Differential Attenuation and Dual-Ended Measurement

Due to bends, connectors, splices and other irregularities the differential attenuation ($\Delta\alpha$) from (2.8) does not remain constant along the fiber [9]. Dual-ended measurement DTS systems allow for the differential attenuation to be resolved directly for each desired measurement location. This allows for much more accurate temperature profiles to be generated than with single-ended measurement techniques where the differential attenuation is assumed constant along the fiber. For dual ended measurements, a single fiber loop is measured by the DTS. At one end the fibers are connected to two separate channels of the DTS and at the other end the fibers are spliced together. This allows the DTS to send laser pulses in either the forward or reverse directions through the loop.

Each measured point is measured once in the forward and once in the reverse direction. For a fiber optic cable of length $\frac{1}{2} L$ the resulting loop created by the splicing two strands will be L . A measured location z in the forward direction will be at $L-z$ when measured from the reverse direction. Figure 2.8 shows the basic configuration for dual-channel measurement of a single fiber.

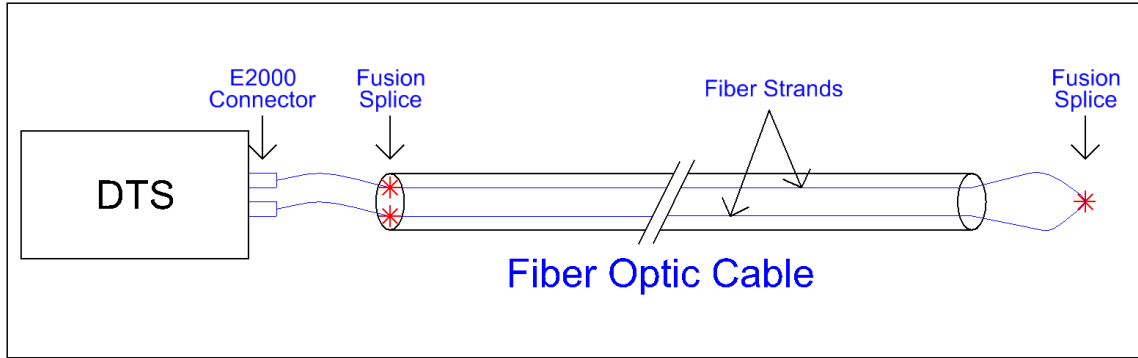


Figure 2.8: DTS Dual Channel Measurement

Assuming that the time interval between forward and reverse measurements is sufficiently small so that the temperature at measurement location z remains constant, the time dependence of (2.8) may be ignored yielding the following equations for fiber temperature as taken in the forward (z) and reverse ($L-z$) directions [9].

$$T(z) = \frac{\gamma}{\ln\left(\frac{P_s(z)}{P_{as}(z)}\right) + C - \int_0^z \Delta\alpha(z') dz'} \quad (2.9)$$

$$T(L-z) = \frac{\gamma}{\ln\left(\frac{P_s(L-z)}{P_{as}(L-z)}\right) + C - \int_L^{L-z} \Delta\alpha(z') dz'} \quad (2.10)$$

By setting (2.9) and (2.10) equal, the differential attenuation $\Delta\alpha$ can be found algebraically over distance Δz and is shown below in (2.11) [9].

$$\int_z^{z+\Delta z} \Delta\alpha(z')dz' = \frac{\ln\left(\frac{P_s(z+\Delta z)}{P_{as}(z)}\right) - \ln\left(\frac{P_s(z)}{P_{as}(z)}\right) + \ln\left(\frac{P_s(L-z)}{P_{as}(L-z)}\right) - \ln\left(\frac{P_s(L-z+\Delta z)}{P_{as}(L-z+\Delta z)}\right)}{2} \quad (2.11)$$

By stepping along the entire length of the fiber in steps of Δz , and summing the values of $\Delta\alpha$, an estimate for the differential attenuation from the DTS to the any measurement point can be calculated. In Chapter 5 the results of single- and dual-channel measurements are compared using a controlled testing environment.

2.5.3. Optical Fiber Construction

Optical fibers are constructed according to their intended applications. The main defining factors for optical fiber cables are the core and cladding diameters and the frequency range for which they are designed. The core and cladding dimensions are typically given in micro meters, also known as microns, and are listed as core/cladding microns. Fibers which are meant to carry only a specific light frequency are known as single-mode (SM) and those designed to carry a range of frequencies are called multi-mode (MM) fibers. The DTS used for data collection in this work was designed to operate using 50/125 micron MM fibers.

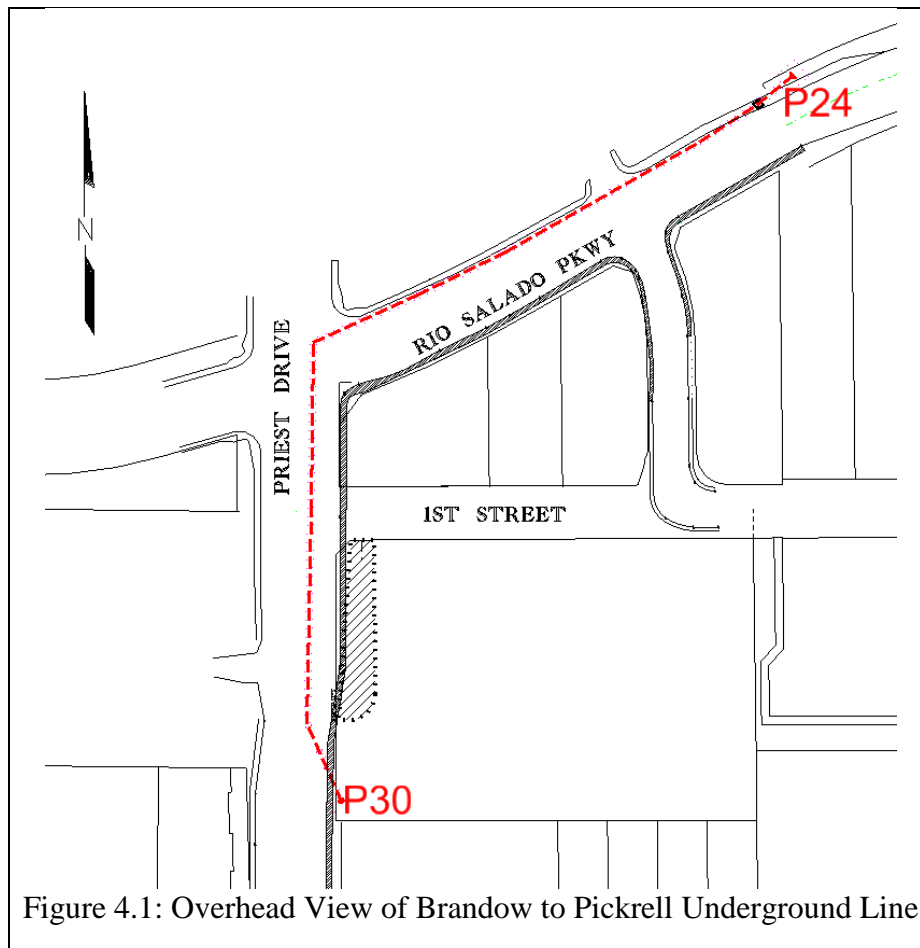
3. SELECTION OF MONITORED UNDERGROUND (UG) LINE

With sixteen installed 69 kV underground circuits it was not clear initially which line would be the best choice for monitoring. It was desirable to use a line that had a relatively large range of loading and also one that would not pose too many obstacles to installation of monitoring equipment and/or sensors. The first choice was the underground portion of the line connection substations Papago and Buttes. This line was the original choice for its heavy loading, long underground length (3500 ft), higher than usual burial depths and interesting underground terrain. However, during the preliminary research stages of using the Papago-Buttes UG line it was discovered that in 2002 SRP had used UG 69 kV cables with (preferable) embedded optical fibers on the installation of the Brandow to Pickrell UG line. The optical fibers were located in the jacket of the UG cables. By using DTS, this would allow for the most accurate and real-time measurements of cable temperatures. The Papago-Buttes installation would require installation of thermocouples or optical fiber into one of the spare duct bank conduits which would yield distorted measurements that would require estimation of conductor temperatures based on approximate thermal models. Using the Brando-Pickrell installation was the better choice not only for achieving more accurate results but also for reduced cost since the temperature probes (the fiber) were already installed. Only the monitoring equipment needed to be purchased and installed.

4. BRANDOW – PICKRELL EXISTING INSTALLATION

4.1 Overview

The Brandow – Pickrell 69 kV transmission line consists of two overhead and one underground section which together connect SRP owned substations Brandow and Pickrell. The underground section connects the overhead conductors which terminate at SRP riser poles P24 and P30 located at the N-E and S-E corners, respectively, of Rio Salado and Priest Dr. in Tempe AZ. Figure 4.1 shows an overhead view of the underground path of the Brandow to Pickrell underground line.



The UG circuit consists of six (two per phase) 1500MCM high voltage cables manufactured by Nexans of Germany. Each cable contains six 50/125 micron MM optical fibers. When the installation was constructed in 2003 the optical fibers of the Nexans cables were spliced at the riser pole insulators to six-strand, riser grade, 62.5/126 micron MM optical fibers manufactured by Corning Optical. The Corning cables were brought down the riser poles to termination boxes approximately ten feet from the riser pole's base. Approximately thirty feet of spare fiber for each UG cable was left inside the termination box at P24 and P30. Figure 4.2 shows the fiber splice box (right) on riser pole 30.



Figure 4.2: Riser Pole 30 Fiber Splice Box

4.2 Duct Bank Configurations and Materials

Various configurations were used in the duct bank construction along the underground path. Figure 4.3 and Figure 4.4 show the underground profile. Different duct bank configurations are denoted by color change and corresponding labels above each section.

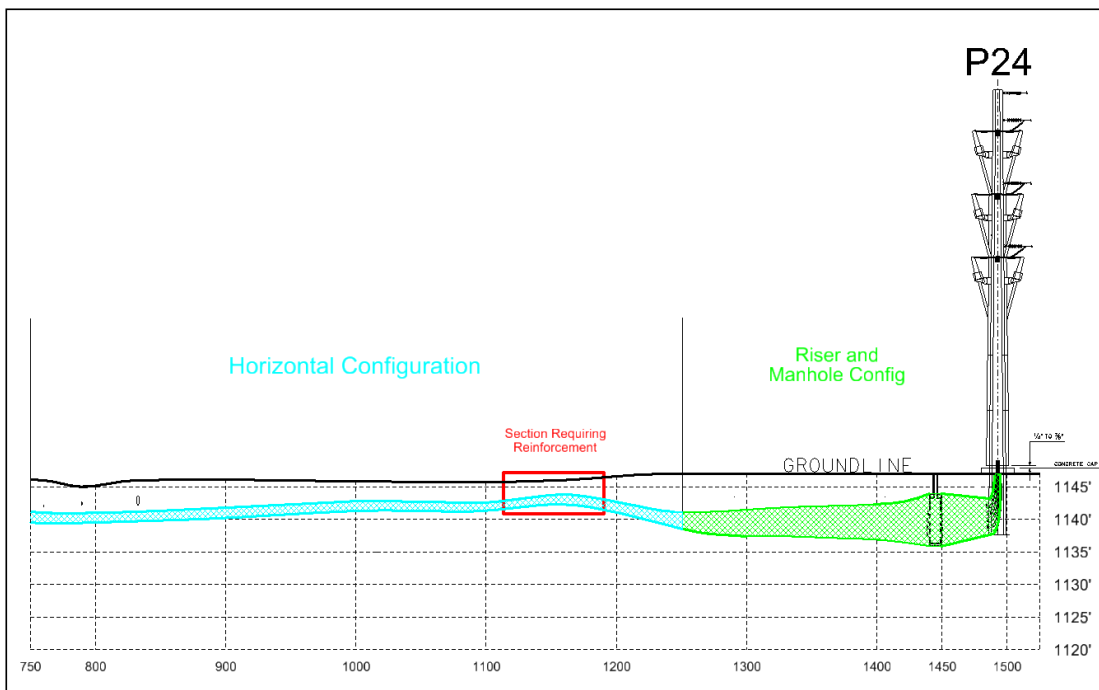


Figure 4.3: UG Duct Bank Profile - Section A

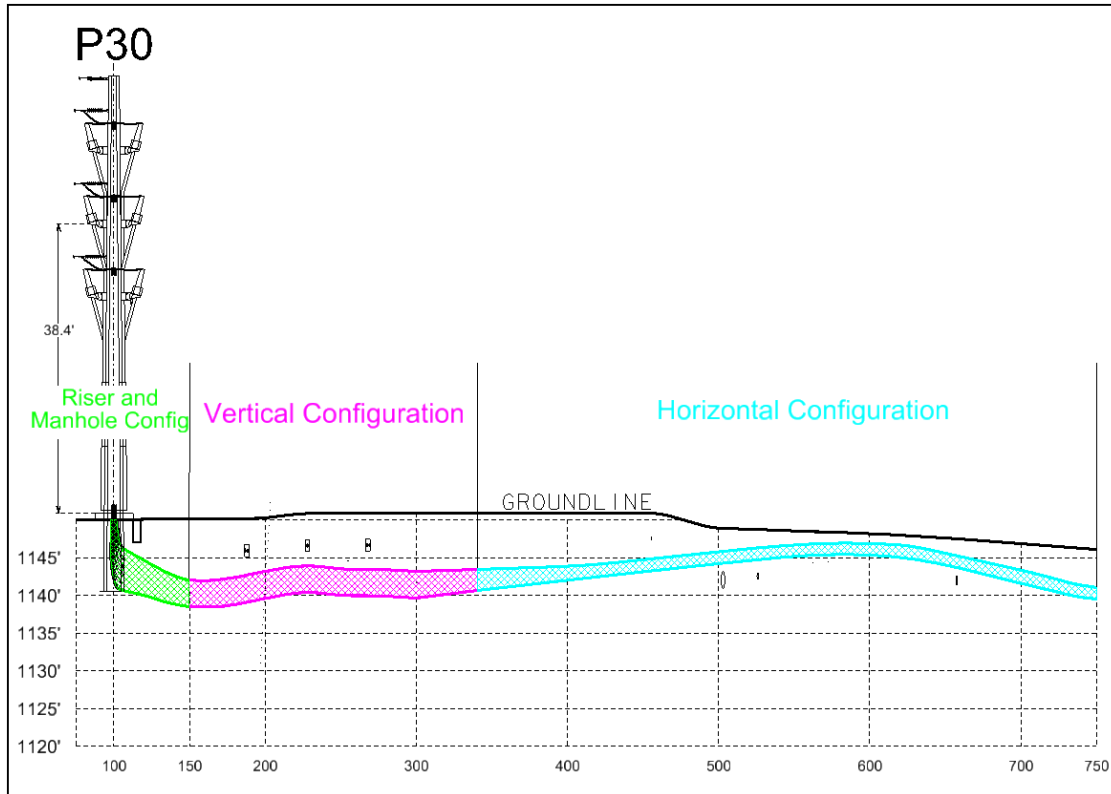


Figure 4.4: UG Duct Bank Profile - Section B

The underground profile consists of three main duct bank configurations; horizontal, vertical, and vertical at manhole and riser poles. Cross-sectional views of each configuration type can be seen below in Figure 4.5, Figure 4.6 and Figure 4.7.

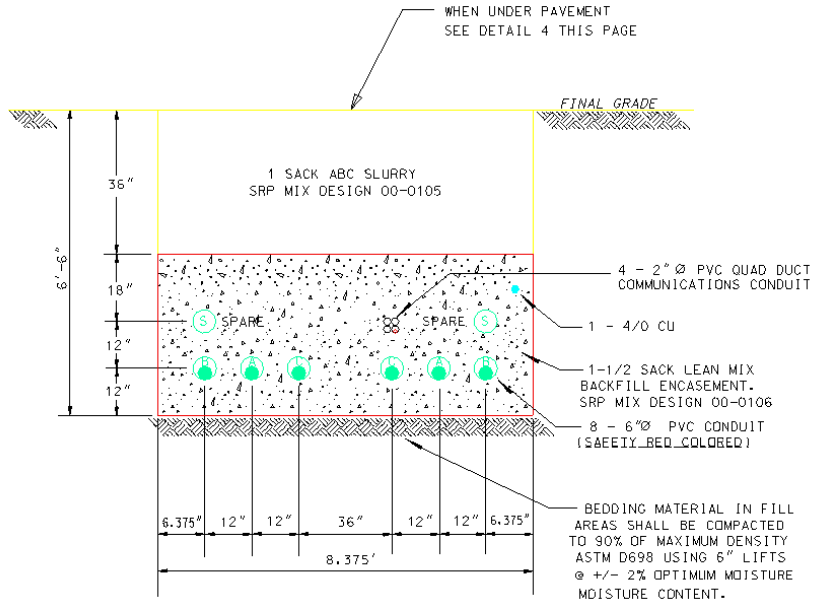


Figure 4.5: Horizontal Configuration [3]

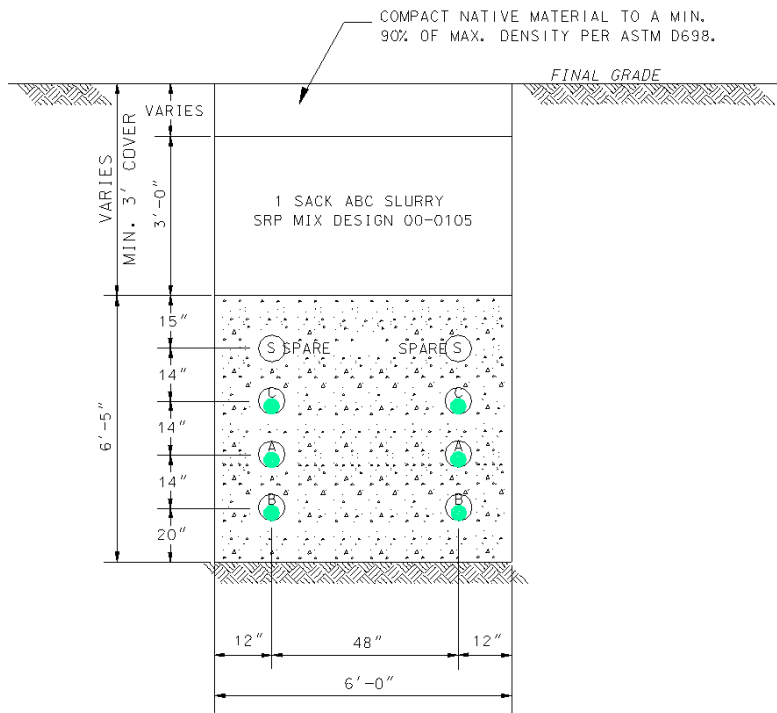


Figure 4.6: Section at Manhole and Riser Poles [3]

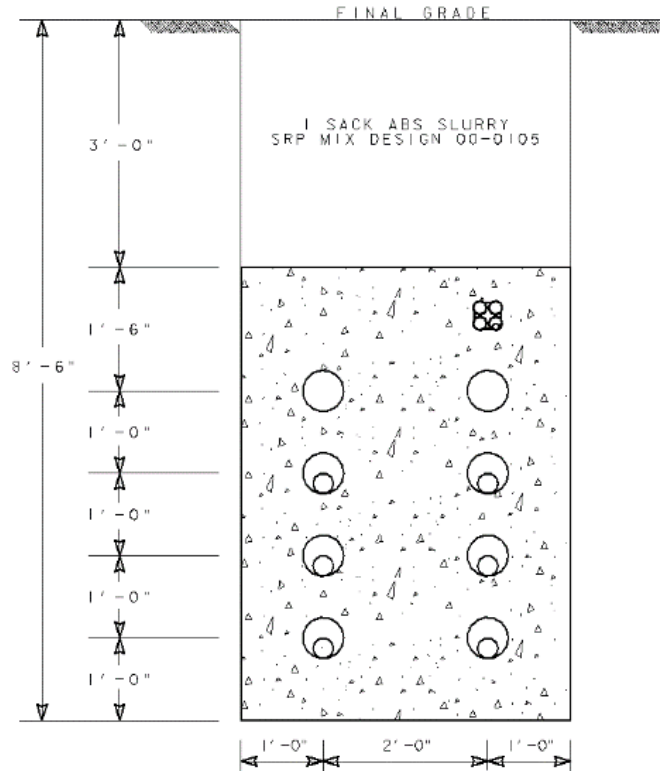


Figure 4.7: Vertical Configuration [3]

The duct banks are constructed of a medium density concrete and consist of eight 6-inch PVC conduits and four 2-inch PVC conduits. Six of the 6-inch conduits are used for the high voltage electric power cables (two per phase) and two are spares which could be used for cable replacement or unforeseen future need. The 2-inch conduit is used for low-voltage copper, and fiber-optic communications cabling.

4.4 Existing (assumed) Hot Spot Location and Cable Ampacity

For the original ampacity calculations the deepest portion of the underground path was selected as the hot-spot location. This location also crossed beneath another high-voltage underground transmission line operated by Arizona Public Service (APS) and can be seen in Figure 4.9. The APS line is a 230 kV underground circuit and uses one conductor per phase.

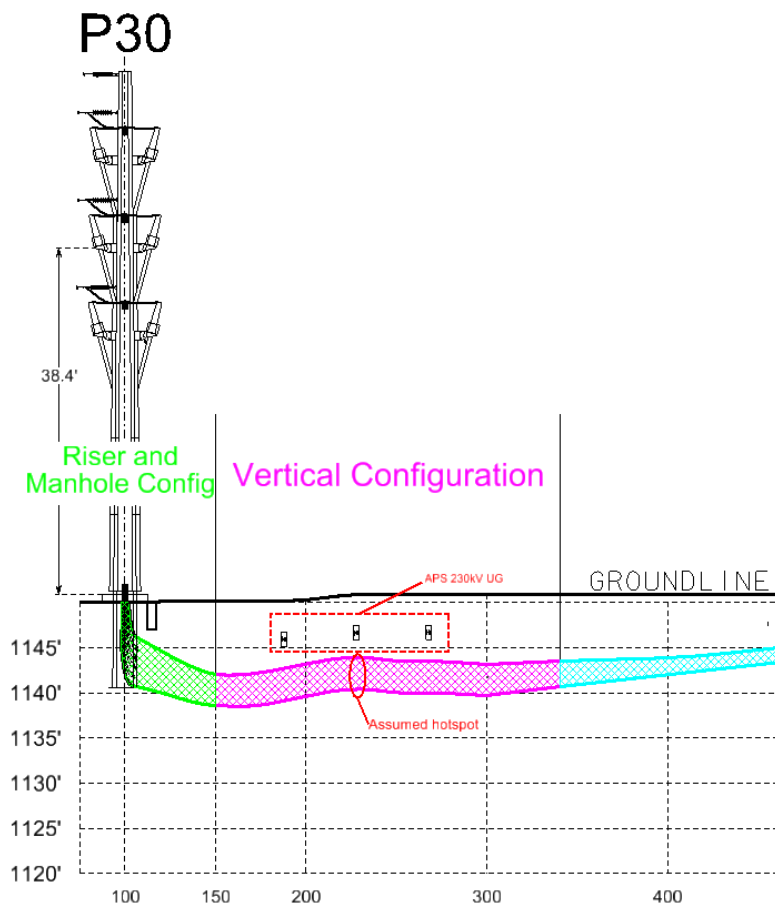


Figure 4.9: APS 230kV UG Line Crossing With Brandow - Pickrell Line

Using the geometry of this assumed hot spot, an ambient temperature of 35 °C and two conductors per phase the original steady-state ampacity of 1600 A and a 300 hour emergency rating of 1900 A were assigned when the line was first commissioned. The original ampacity calculation was done using traditional closed form solution analysis based on the Neher-McGrath [4] method. The original calculation results can be found in reference source [3].

5. DTS LABORATORY TESTING

The DTS unit is designed for use with 50/125 micron optical fibers. However, the Brandow – Pickrell installation posed a unique situation where the fibers in the measured underground cable were of the correct specification but connected at each end to jumper fibers with a larger core diameter of 62.5 micron. Since the DTS manufacturer was uncertain of the effects the mismatched fibers would have, it was necessary to validate the accuracy of the DTS measurements before attempting to collect any underground cable temperature data. A laboratory testing setup to simulate the Brandow-Pickrell UG installation was constructed at an SRP warehouse facility. Two sections (A and C) of six strand-riser-grade 62.5/125 micron fibers were used to simulate the jumper fibers on riser poles 24 and 30. The integrated fibers of the Nexans UG cable were simulated by a six-strand, reinforced 50/125 micron fiber optic cable (section B). Only two of the available six strands were used from each section. Section A was connected to Section B by fusion splicing two color matched fiber strands. The same was done to connect section B to C. The two strands were spliced together at the end of section C and at the beginning of section A they were spliced to E2000 connectors. The result was a single fiber loop consisting of three distinct sections that accurately represented the Brandow – Pickrell UG line. A graphical representation of the test setup can be seen in Figure 5.1.

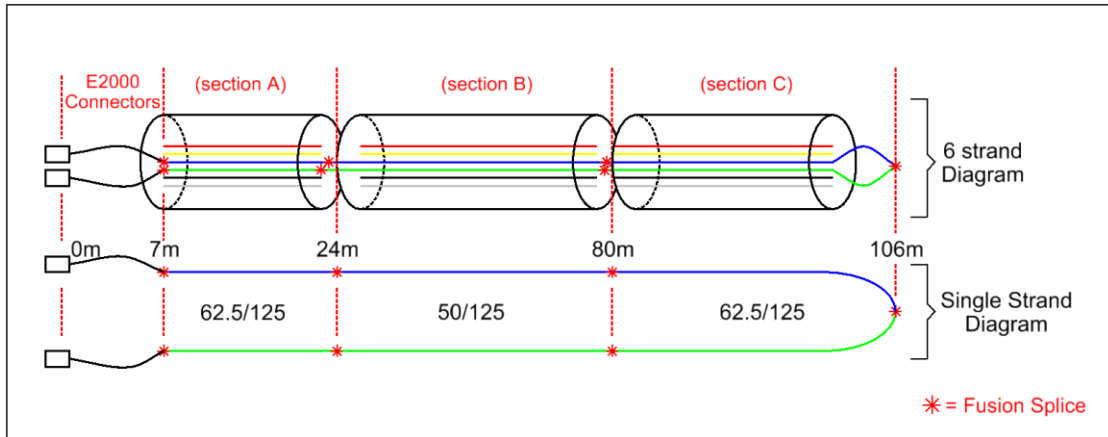


Figure 5.1: Test Setup Simulating Brandow – Pickrell Fiber Optic Arrangement: Section A represents the splice fiber on riser pole 24; Section B represents the Nexans UG fiber; Section C represents the splice fiber on riser pole 30. The E2000 connectors are connected to channels 1 and 2 of the DTS.

5.1 Laboratory Test Setup

The arrangement shown in Figure 5.1 was to be used determine the effects of mismatched fiber core diameters, like those of the Brandow-Pickrell UG line, on the DTS measurement accuracy. Each section was coiled and placed into individual plastic containers with a thermocouple placed inside to collect reference temperature data. A diagram of the testing setup can be seen in Figure 5.2. The boundaries of each section were precisely located using Optical Time Domain Reflectometer (OTDR) data provided by the DTS. The OTDR data shows the power in decibels of the received Stokes and anti-Stokes backscattered light. The step change in attenuation due to the splices between different fiber strand diameters made it easy to identify the individual fiber sections.

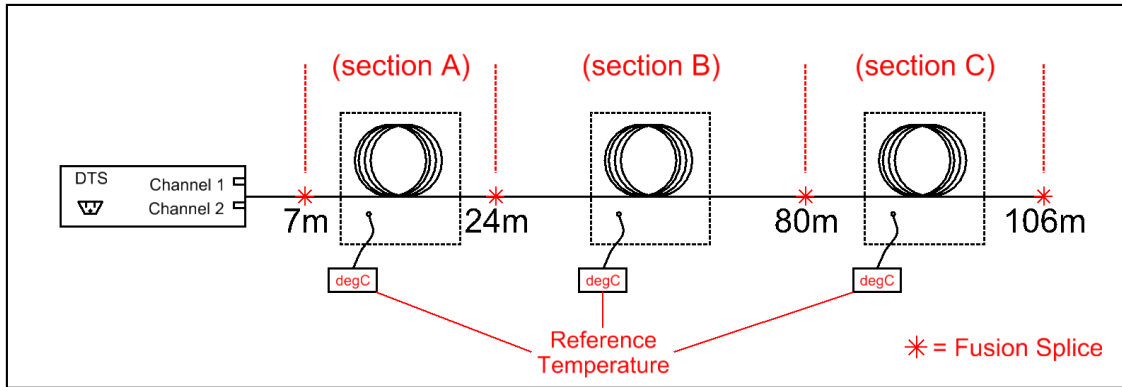


Figure 5.2: Test Setup With Coiled Reference Temperature Sections

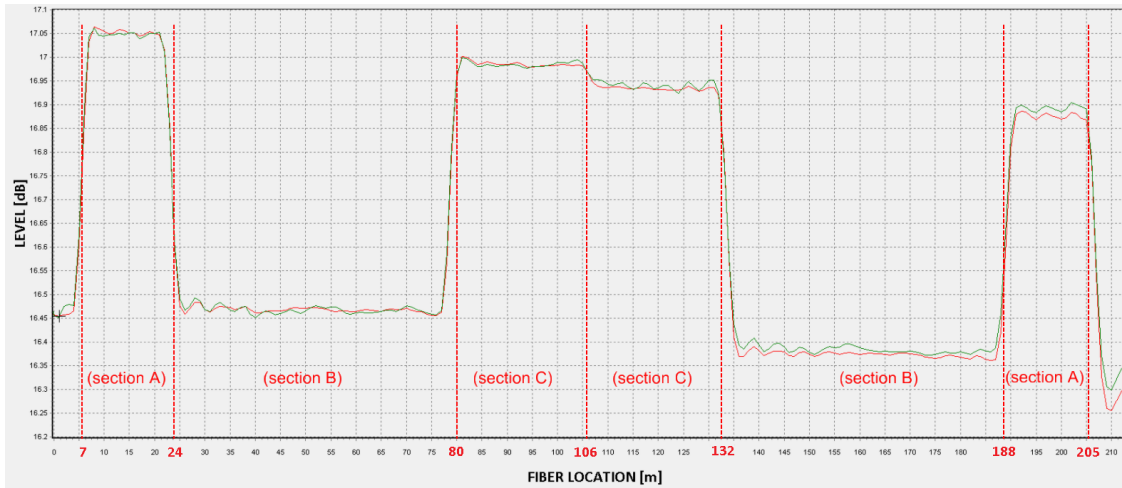


Figure 5.3: DTS OTDR Showing Boundaries for Each Fiber Section

Figure 5.3 shows the OTDR resulting from a scan of the entire loop created by splicing the individual strands from cable sections A, B, and C. The Stokes backscatter is displayed in red and the anti-Stokes in green. The larger core diameters of sections A and C result in a higher magnitude of the received Stokes and anti-Stokes components relative to the smaller core fibers of section B. It can be seen that each section is represented twice in a single OTDR scan due to the loop configuration.

5.2 Laboratory Test Results

DTS measurements were taken for each coiled section and compared to their corresponding reference temperatures. In order to avoid measurement distortion due to connectors or fusion splicing, the temperature of each section was represented by taking the average temperature over the center 30 percent of each coil. Figure 5.4 shows the DTS temperature trace taken over a 20 meter span at the center of fiber section B. The minimum, maximum and average temperature over the displayed distance is also highlighted in Figure 5.4.

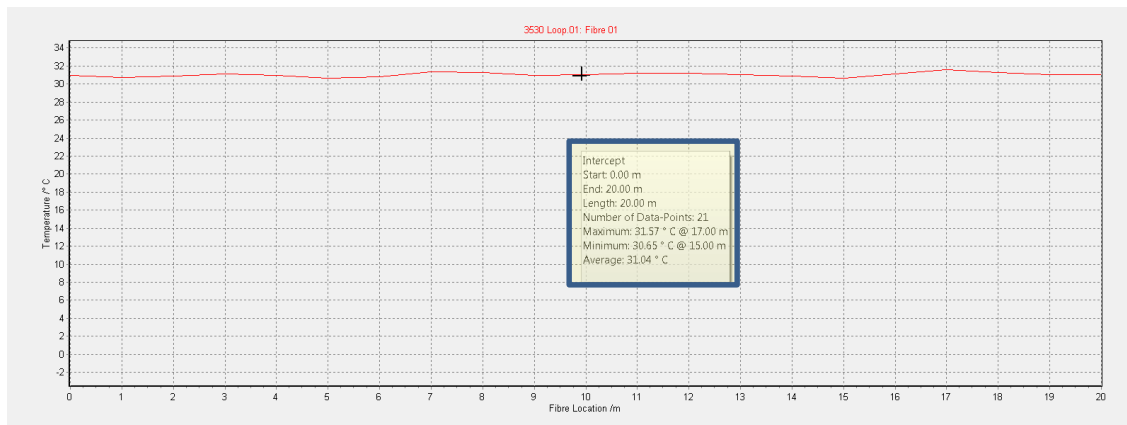


Figure 5.4: Section B DTS Trace - Reference Temperature at 31.1°C

Table 5.1: Test Setup Results

	Measurement Time [s]	Spatial Resolution [m]	Fiber Section	Average [C]	Max/Min [C]	Reference [C]
Dual Ended	60	1	B	31.04	31.57/30.65	31.10
Single Ended	120			32.59	33.01/32.00	

The same procedure was repeated for sections A and C. The procedure was also repeated with section B being submerged in a water and ice solution. Table 5.1 shows the average (column 5) and maximum/minimum (column 6) DTS temperature over the center 20 meters of Section B using both Single-Ended and Dual-Ended measurement mode. The measurement times (column 2) represent the total time over which the DTS measurements were made. The measurement time listed is the measurement time per channel; thus the total measurement time for both Dual and Single-Ended measurements is effectively 120 seconds. Table 5.1 shows the average temperature taken using Dual-Ended measurement mode was only 0.06 °C less than the reference temperature reading (column 7) which is well within the rated ± 1 °C rating of the DTS. Table 5.1 shows that by using single-ended measurement mode over the same section the average temperature varied by nearly 1.5 °C. These results confirmed that by using dual ended measurement configuration the effects of the mismatched fiber diameters could be negated and the temperature accuracy of the DTS maintained within its rated tolerance. Conversely, it was shown that temperature calibration was needed for single ended measurements. While the use of single channel measurements may be applicable in some situations, the inability to accurately take reference temperature readings from the UG cable in the case of this research makes single channel measurements an unreliable and impractical solution. It was decided from this experiment to use the dual channel measurement configuration for the Brandow – Pickrell UG data collection.

6. DTS INSTALLATION

This section details the physical construction at the DTS installation location as well as the initial commissioning process. It is included to serve as a guide and lessons learned for SRP or other utilities installing DTS monitoring systems in the future. To understand the interpretation of the results section (provided in Chapter 9) it is not necessary to read this chapter.

The proposed installation location for the DTS system was in a shaded area approximately 3 feet to the east of the concrete base of riser pole 24 (see Figure 6.1). The DTS system required a secure, climate controlled environment with an electrical power source, neither of which was available at the installation site. This section lists and describes the necessary work completed that allowed for the on-site installation and commissioning of the DTS system.



Figure 6.1: DTS Enclosure Installed Next to Riser Pole 24

6.1 NEMA Rated Outdoor Enclosure

Due to the harsh outdoor environment and high temperatures of Phoenix, it was decided to mount the DTS system in an insulated and air-conditioned NEMA (National Electrical Manufacturers Association) Type 4, outdoor enclosure which can be seen in Figure 6.2. The enclosure was purchase with an attached mini air-conditioner which required a 120 Volt ac power source. SRP provided a fiberglass distribution transformer pad to be used as a mounting base for the enclosure.



Figure 6.2: NEMA Rated Outdoor Enclosure for DTS System

6.2 AC Power Connection

Both the DTS and the mini air-conditioner required 120 V ac which was not readily available at the installation site. After some investigation it was discovered that an SRP streetlight circuit (120/240Vac split phase) ran just beneath the sidewalk to the south of the riser pole. It was decided to remove a section of sidewalk nearest to the DTS enclosure and tie into the existing streetlight circuit. A new junction box was installed between the sidewalk and the enclosure location and a new underground conduit was installed allowing power to be brought into the base of the DTS enclosure.



Figure 6.3: Conduit Trench for AC Power Cable to DTS

6.3 Fiber-Optic Cable Installation, Identification, and Splicing

The fiber optic cables needed to be brought from the junction box on the riser pole to the opening in the base of the DTS enclosure. A riser molding cover was used to bring the fiber from the junction box approximately 10 feet to the concrete base of the riser pole. Flexible conduit was buried between the concrete base and the enclosure. To protect the flexible conduit where it was exposed at the riser pole base, it was covered with a quick setting concrete.

Once the fibers were brought into the DTS enclosure it was not known which underground power cable each fiber was associated with. It was not practical to physically trace out each fiber since it would require coming into close proximity with live 69 kV lines or requesting that the line be de-energized. Instead each fiber was identified by using the length markings printed on the jackets of each cable. This required that the length marking be read from five of the six fiber optic cables ascending from the DTS to the HV insulators on riser pole 24. The highest insulator was at approximately 48 feet from the base of the pole and the cable length markings were less than one inch in height. In order to read the length markings at this distance, a digital camera with optical image stabilization and a telephoto lens was used. The recorded length markings, observing whether the length markings were ascending or descending combined with the approximate length of each of the fiber optic cables allowed for each cable to be precisely identified. Figure 6.4 shows the length marking on the riser-grade fiber optic cable taken at a distance of approximately 30 feet.



Figure 6.4: Length Markings on Corning Fibers

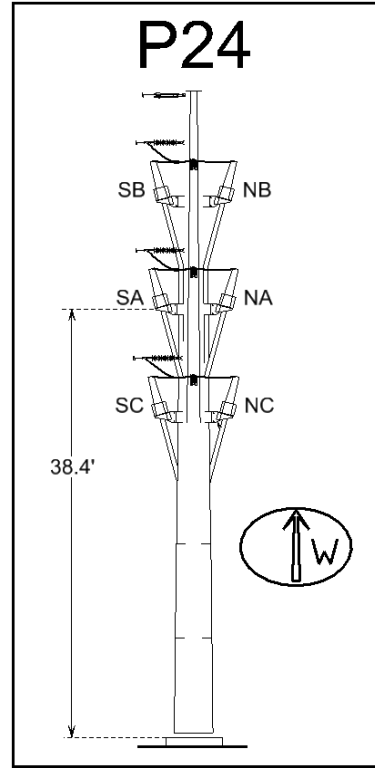


Figure 6.5: Diagram Showing the Label Associated with Each UG Cable

Once each cable was identified it was labeled with a unique identifying mark determined by the north/south orientation and phase of its connected underground cable. Figure 6.5 shows a diagram indicating the labels that can be found on each fiber optic cable inside the DTS enclosure beside the underground cable it is connected to.

At the DTS enclosure, two E2000 connectors were spliced to each of the six fiber-optic cables and remarked with the identifying mark described above. At the other end of the underground line, at riser pole 30, two fiber strands from each cable, those associated with the E2000 connectors, were spliced together forming 6 separate fiber loops, one for each UG cable. Each fiber loop was a full-scale version of the test setup described above in section 5.1.

7. EXPERIMENTAL SETUP

A Distributed Temperature Sensing (DTS) system was installed on the Brandow-Pickrell underground 69 kV circuit. The underground circuit consists of two 1500 MCM cables per phase, each with integrated optical fibers in the cable jackets. The DTS was installed in an outdoor NEMA rated cabinet beside one of the underground riser poles (P24). The integrated fibers on each underground power cable were spliced to individual riser grade fiber optic cables at the underground/overhead insulators and brought down the riser poles at either end of the circuit. The fibers were connected so that dual ended measurements (2.5.2) could be made on each underground cable.

7.1 Measured Cable/Phase and Fiber Connection

Cable SA was selected for measurement because it is the center phase throughout the underground path and as such is expected to have higher relative temperatures. A schematic of the fiber connection for cable SA can be seen in Figure 7.1 and an overview of the fiber path can be seen in Figure 7.2.

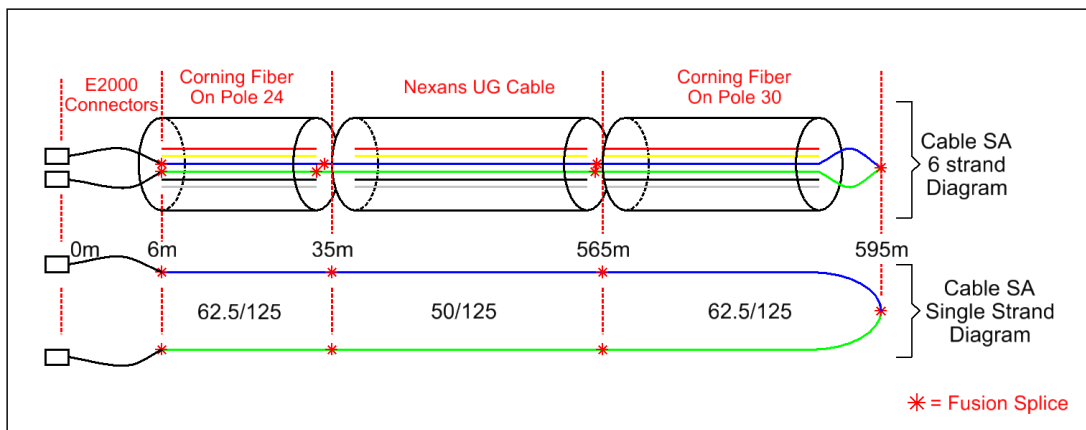


Figure 7.1: Brandow-Pickrell Fiber Optic Configuration

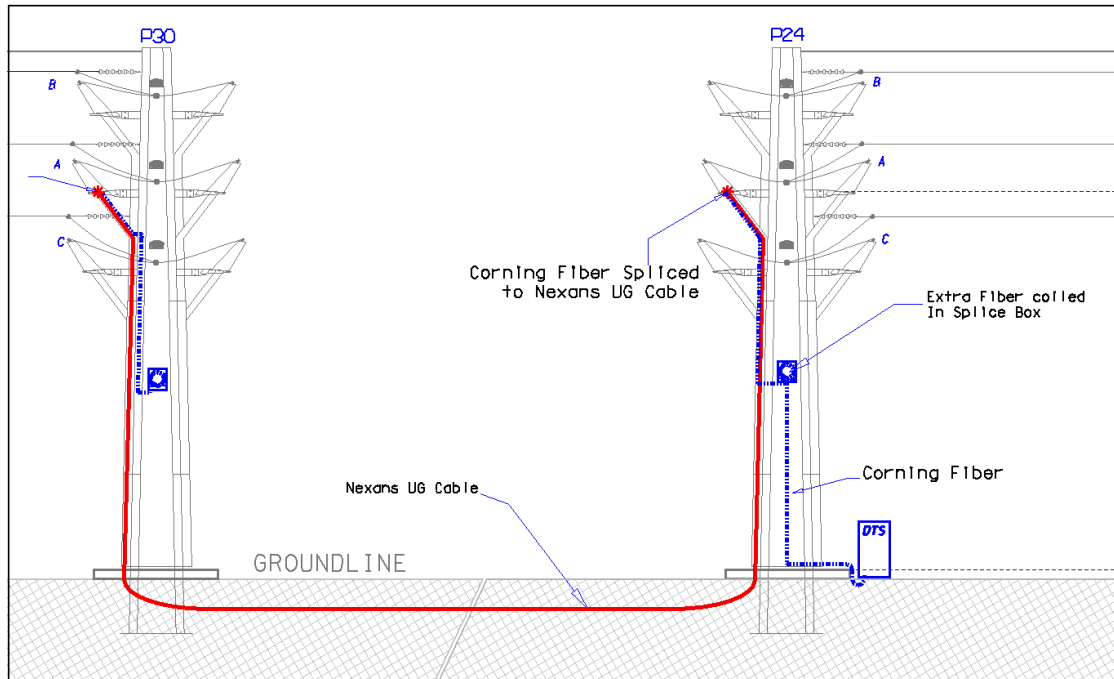


Figure 7.2: Brandow-Pickrell UG Cable SA Path

7.2 Length of Underground Cable

In order to relate measured data taken from the underground cable it was crucial to have a reliable estimate of the cable distance and a map of the underground profile which could be compared to the DTS measurements. Since the exact installed lengths for each UG cable were not known it was necessary to estimate the lengths using the as-built installation data and field measurements. The length of the underground

section was estimated by creating a scale, CAD drawing of the Brandow-Pickrell UG line and measuring along the cable path with one of the built in CAD measurement tools. The riser section heights were directly measured using a laser range finder and the measured distance was used to correctly scale the CAD representations of riser poles 24 and 30. The total estimated length of cable SA (see Figure 6.5) was determined by adding the above ground riser section lengths to the estimated length of the UG section. The total estimated length of the Nexans underground power cable connected to measured fiber (SA) was 1489 feet.

8. DTS COMMISSIONING AND PRELIMINARY RESULTS

The DTS was rack-mounted into the outdoor enclosure described in section 6.1 on January 16th 2015. The DTS was connected to the newly installed ac power source and the optical inputs (Chanel 1 and Chanel 2) were connected to the E2000 connectors on cable SA. The DTS needs to be configured each time it is connected to new optical fibers for the first time. This section gives a brief overview of that commissioning process and a review of the initial DTS trace results.

8.1 DTS Commissioning and Charon3 Software

Changes to the DTS configuration are made using a PC computer via a USB connection with the manufacturer-provided software package called Charon3® by LIOS Technology®. Since the DTS needs to be connected to the optical fibers it would be measuring during the commissioning process, a laptop PC with Charon3® software installed was used on-site for the initial setup.

Using Charon3®, the connected fiber loop was scanned from each direction using DTS channel 1 and channel 2. Figure 8.1 shows the resulting length scan of channels 1 and 2 for fiber SA.

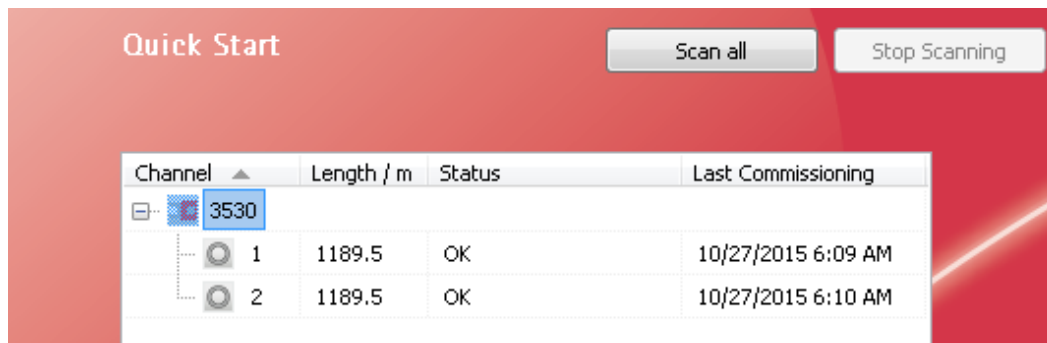


Figure 8.1: Charon3 Quick Start Length Scan of Optical Channels 1 and 2

The length scans of fiber channels 1 and 2 shown in Figure 8.1 are of the entire fiber loop comprised of the Nexans UG power cable and both of the Corning optical fibers on riser poles 24 and 30. Also, since the fibers along the Nexans cable are wound helically (as described in section 2.1.5) the resulting length scan is greater than the actual linear distance of the combined Nexans and Corning cable sections. The DTS length scan cannot be directly used to estimate cable lengths. The process of scaling and adjusting the raw DTS data to align with the underground power cable is shown in section 8.3.2. If the length scan shows that the length of fiber connected to both channel 1 and 2 is equal Charon3® will allow the user to use the Dual-Ended measurement mode which is listed as “Loop Configuration”.

By default the DTS measurement parameters call for the entire length of connected fiber to be measured with a spatial resolution of 1[m] and a measurement time of 30 seconds. These initial settings were used to acquire an initial temperature trace and backscatter profile which were used to determine the appropriate adjustments to the measurement parameters. Figure 8.2 shows the backscatter scan of fiber loop SA with the Stokes component displayed in red and the anti-Stokes in green.

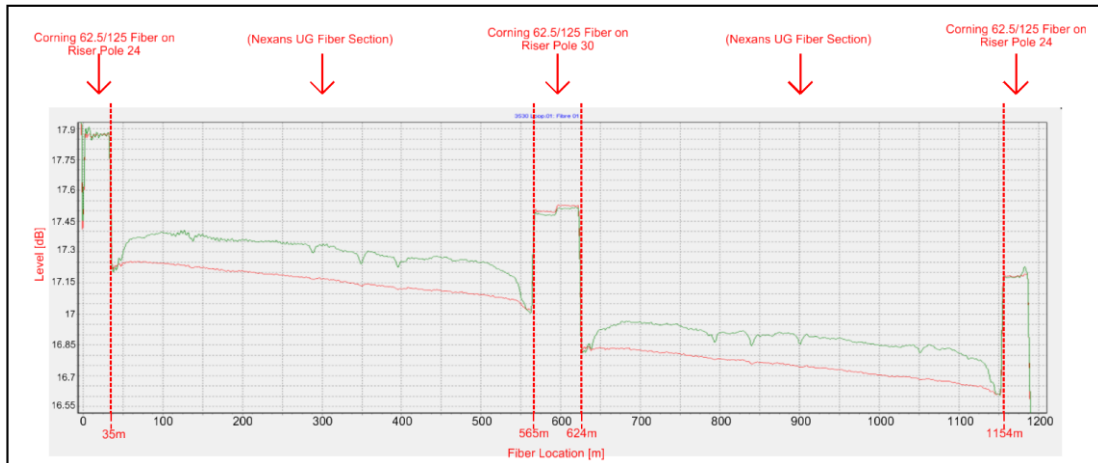


Figure 8.2: Backscatter Scan of Fiber SA

Discontinuities in the magnitudes of the backscatter components occur at 35, 565, 624 and 1154 meters and are due to splices between the embedded fibers of the Nexans UG cable and those of the Corning optical fibers. The section of Corning fiber that extends down riser pole 30 is identified in Figure 8.2 between 565 and 624 meters. The smaller discontinuity in backscatter attenuation seen near the center of this section (595 meters) is caused by the splice between the two strands of the Corning fiber-optic cable. This point marks the start point for the return half of the fiber loop. Any temperature readings taken from this point onward would be redundant and thus are excluded from the trace range of the DTS. Figure 8.3 shows the initial DTS temperature trace of the entire 1189.5 meter loop and it can be seen that the data are roughly symmetrical about the 594 meter point which corresponds to the loop midpoint fiber splice. Data reported from further temperature scans only include data from 0 to 594 meters.

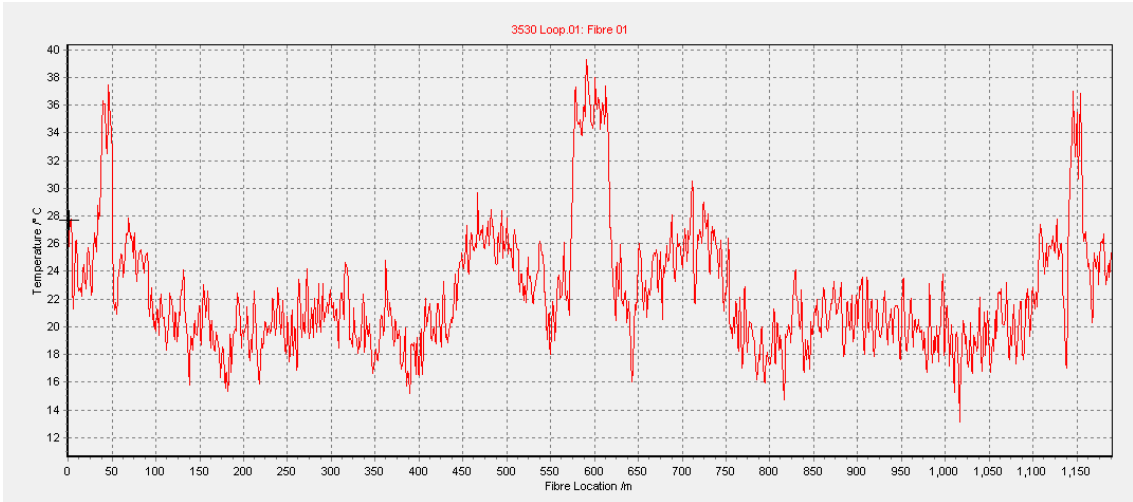


Figure 8.3: Temperature vs Distance for Complete SA Loop

The final measurement configuration can be seen in Figure 8.4 and in Table 8.1 a description of each setting is shown.

The screenshot shows the 'Measurement Parameter Sets - Loop.01: Fibre 01' dialog box. The title bar includes a close button. The main content area is titled '3530 - Loop.01: Fibre 01' and contains the instruction 'Setup measurement speed and measurement resolution of the selected fibre.' The settings are organized into three sections:

- Measurement:** Sampling Interval is set to 1.00 m, Measuring Time is 150 s. There is an unchecked checkbox for 'Fast Measuring Mode'.
- Processing:** Averaging is set to 2, and Reference Point is 0.00 m.
- Data Transmission:** Temperature Profile Start is 0.00 m, Temperature Profile End is 594.00 m. 'Send Each x. Curve' is set to 1, and 'Transmit Backscattering Profile' is checked.

At the bottom, there is a table with columns: Name, Sampling Interval / m, Measuring Time, Maximum Fibre Length / m, and Fast ... The table is currently empty. Below the table are buttons for 'Assign', 'New', 'Copy', 'Delete', and 'Rename...'. At the very bottom, there is a checked checkbox for 'Show Advanced Options' and 'Cancel' and 'OK' buttons.

Figure 8.4: DTS Measurement Parameters for Cable SA

Table 8.1: DTS Measurement Parameters

SETTING	DESCRIPTION
Sampling Interval [m]	Sets distance between measured points
Measuring Time [s]	Duration of each temperature trace
Averaging (1,2,..10)	Up to 10 temperature measurements for a single point can be averaged for greater temperature resolution.
Reference Point	Sets the selected point to be reference point (0 m)
Temperature Profile Start	Starting position for recorded data
Temperature Profile End	Ending position for recorded data
Send Each x. Curve	Interval value determining how often trace data will be stored. A setting of 2 will result in every other trace to be stored in memory.
Transmit Backscatter Profile	Selecting will result in the backscatter profile for each trace to be stored in memory

8.2 Data Collection

The DTS was programed to take a temperature trace every 5 minutes. Each trace consisted of a temperature reading taken each 1 meter starting at the DTS output and ending at the return loop splice on riser pole 30 (the rightmost fusion splice shown in Figure 7.1). This allowed for data to be collected from the entire UG cable as well as ambient temperatures at either riser pole taken from the Corning 62.5/125 micron fibers. Data were stored to an onboard compact-flash card in the DTS unit and downloaded via USB connection at one week intervals.

8.3 Preliminary DTS Results

A preliminary analysis of the DTS temperature trace data was performed to verify temperatures were within expected ranges and to fit measured data with the underground profile maps.

8.3.1 Comparison of Measured Riser Temperatures to Ambient

The analysis of the backscatter data performed in 8.1 showed that DTS trace data from approximately 3 m to 35 m was from the Corning 62.5/125 micron fiber optic cable. To verify that the DTS measurements were within the expected range, temperature data was collected from the Corning fiber on riser pole 24 using the DTS and then compared to recorded ambient temperature from a nearby, SRP owned, temperature data collection site. The position was selected for being a point along the Corning riser fiber (see Figure 7.1) which would not see heating from the 69 kV cables since it was not embedded in the cable and thus would more closely follow ambient temperatures. Figure 8.5 shows the DTS measured temperature and the recorded ambient temperature for the same time period. It can be seen that the measured temperature follows the shape of the daily ambient temperature curve with a positive shift which is due to the difference in collection location, direct sunlight heating and the greater thermal resistance of the fiber cladding and jacket compared to the dedicated temperature probe at the SRP site used to collect the ambient temperature data.

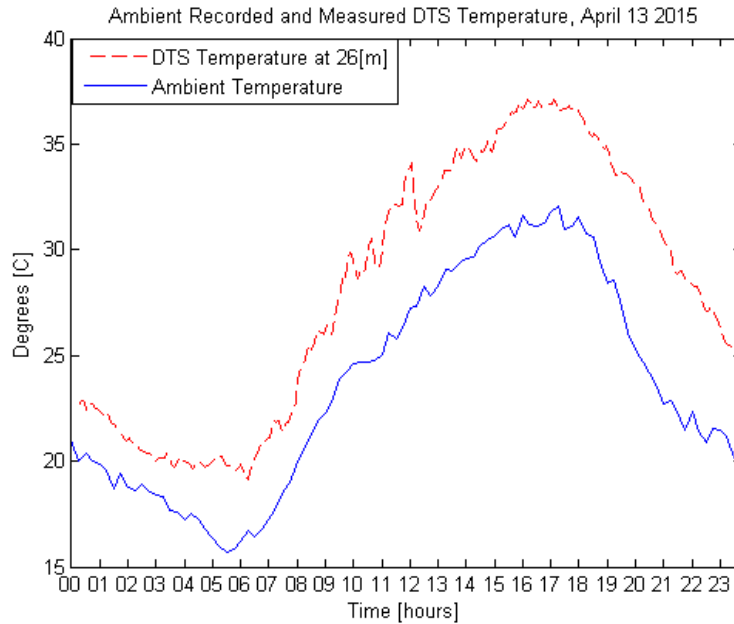


Figure 8.5: Measured Temperature of Corning Optical Fiber 26 meter from DTS

8.3.2 Alignment of DTS Trace Data With UG Profile

SRP provided the as-built installation records for the Brandow-Pickrell UG line which included detailed underground profile maps which were used to construct the CAD representations shown in Figure 4.3 and Figure 4.4. It was decided to shift the DTS collected data so that measurement points (distance from origin) would align with zero-reference on the existing SRP drawings. This would simplify the process of correlating data to the installation geometry since all of the existing drawings used the same measurement units and reference points. In order to align the data collected by the DTS to the provided UG profile several steps were required. First the data needed to be cropped to only include points along the underground cable. Next since the DTS collected data with riser pole 24 being the starting point, it needed to be inverted so the position data would be ascending from riser pole 30 to 24. The data now had to be scaled to align the

points of the helically wound fiber strand with the linear path of the UG cable (see 2.1.5). Using the DTS backscatter data presented in section 8.1 the start and end of the fiber strand embedded in the Nexans UG cable were determined. The backscatter profile for the fiber loop can be seen in Figure 8.6 which shows the starting and ending points for the Nexans UG cable (first half of loop) at 35 and 565 meters. By taking the difference of these two points the unscaled length of the embedded fiber of the Nexans UG cable was found and the calculation can be seen in (8.1).

$$LC_{SA,unscaled} = 565 - 35 = 530 \text{ m} \quad (8.1)$$

This length of 530 meters corresponds to 1731 ft. Taking the $sf=0.86$ into account, this corresponds to the 1489 ft. cable length.

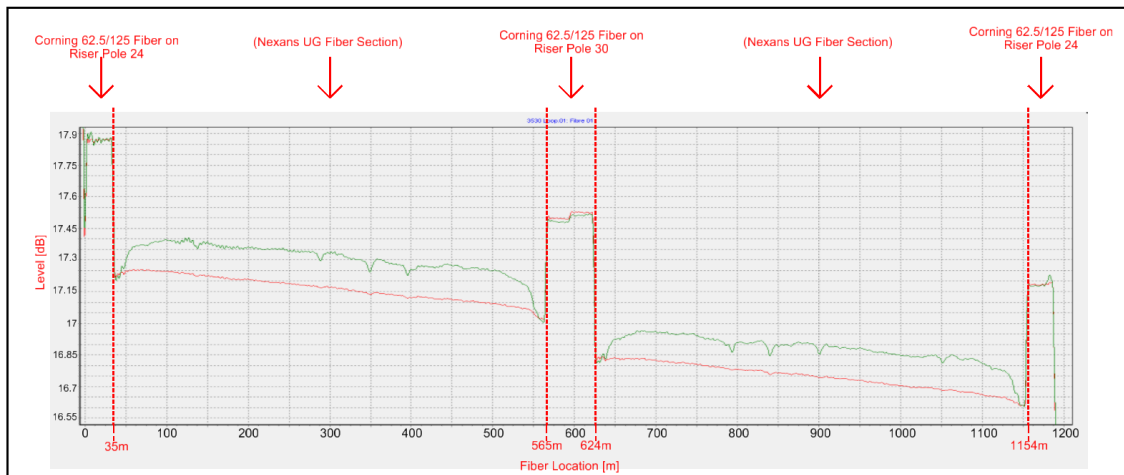


Figure 8.6: DTS Backscatter Data Showing Fiber Splice Locations

The length-of-lay data as described in 2.1.5 was used to determine the appropriate scaling factor (sf) needed to adjust the DTS measurements so that they would correlate to positions along the underground profile map. Equation (8.2) shows the calculated scaling factor.

$$sf = \frac{1}{1.163} \cong 0.86 \quad (8.2)$$

Applying the scaling factor (sf), the calculated linear distance of the UG cable SA is approximately 455.7 m or 1495 feet. The calculated distance of 1495 feet was 6 feet greater than the estimated length of 1489 feet discussed in 0. It was unknown whether the difference between the DTS measured length and the estimated length was due to inaccuracies in the UG profile map, extra fiber coiled at splice locations or some combination of both. Since the distance was relatively small (less than 2 m and the spatial resolution of the DTS is 1 m) and the dimensions at either riser pole were equal, it was decided to split this difference by aligning the DTS measurements with the center of the underground profile. This means that the center of the scaled DTS temperature trace data taken between 35 and 565 meters was aligned with the center point of the UG profile map. Figure 8.7 shows a DTS temperature trace taken on August 15th at 5:32 pm which has been scaled using the scaling factor (sf) and aligned with the SRP UG profile for the Brandow-Pickrell line.

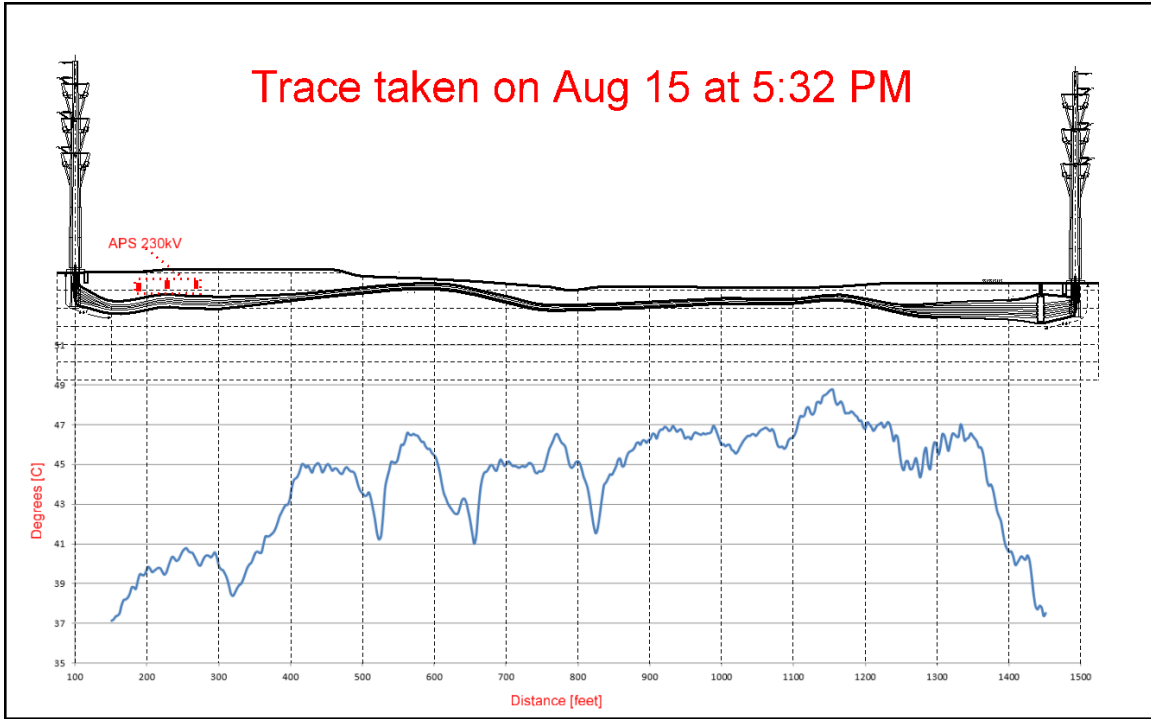


Figure 8.7: DTS Temperature Trace Aligned With SRP UG Profile Map

9. MEASURED RESULTS AND ANALYSIS

9.1 Hot-Spot Locating

The collected DTS trace data included measurements every 1 m along the length of the UG cable and traces were recorded every 5 minutes. By aligning the DTS trace data with the underground profile map provided by SRP it was possible to identify the location of the section of UG line experiencing the highest temperatures relative to the rest of the installation.

A Matlab® code was written to analyze all of the collected DTS data and identify the hot-spot location from each trace. Data from 35 m to 565 m (the beginning and end of the Nexans UG cable) was considered and a total of 57,209 traces were analyzed. In Figure 9.1 the y-axis shows the number of times each x-location was the hot-spot, as a percentage of the total number of traces taken.

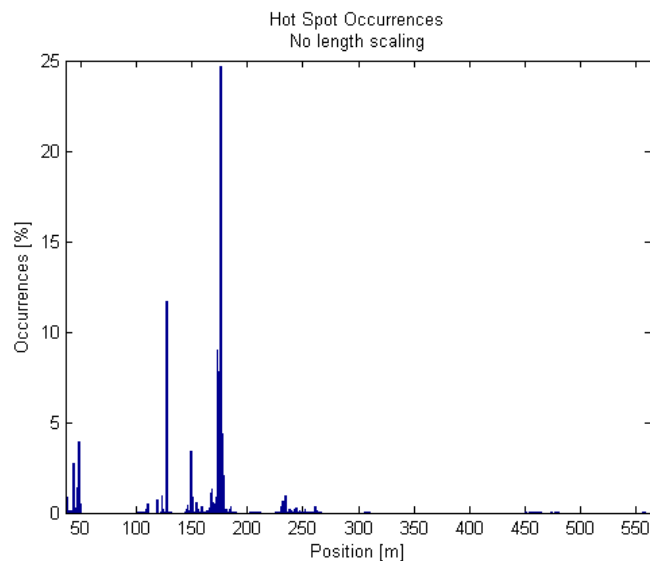


Figure 9.1: Hot-Spot Occurrences between 35 and 565 Meters

In order to relate the hot-spot location information presented in Figure 9.1 to the UG profile the data was scaled and inverted as described in 8.3.2 so that the x-axis locations would correlate to the length markings on the UG profile. The hot-spot data in Figure 9.2 has been aligned with the SRP underground profile map and shows the number of hot-spot occurrences for each location as a percentage of the total number hot-spot occurrences for the UG portion.

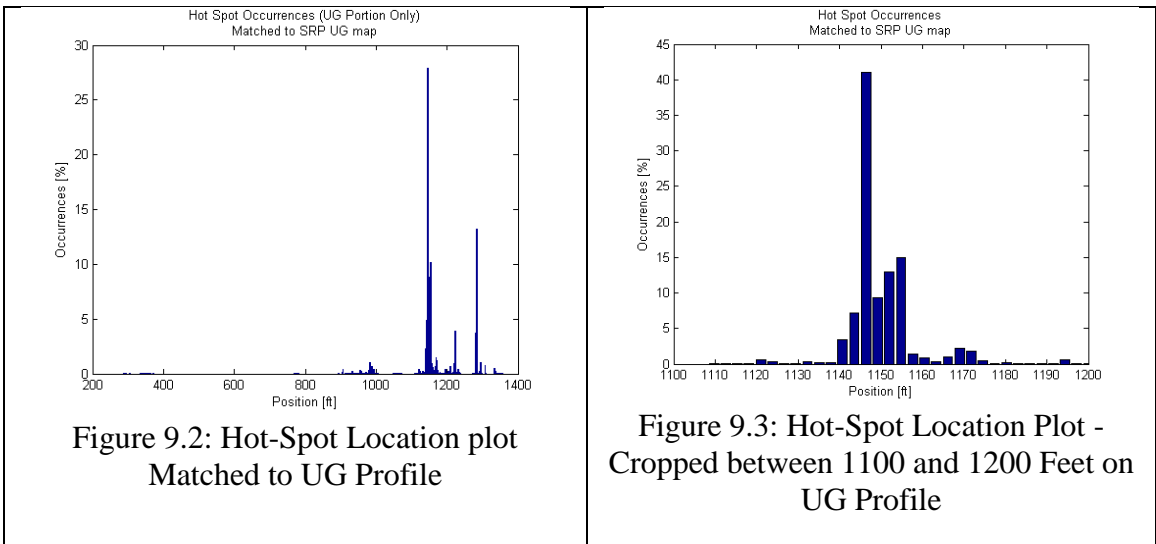


Figure 9.2: Hot-Spot Location plot Matched to UG Profile

Figure 9.3: Hot-Spot Location Plot - Cropped between 1100 and 1200 Feet on UG Profile

Summing the number of occurrences of Figure 9.2 between 1100 and 1200 feet and normalizing by the total number of hot-spot occurrences taken from the entire UG section, it was revealed that 75% of the hot-spot occurrences of the underground portion were collected from this region. Figure 9.3 show the hot-spot locations and occurrences for the UG portion between 1100 and 1200 feet grouped into bins of approximately 3.281 ft (1 m). From this region the greatest number of occurrences occurred at approximately 1146 feet. Based on these results the underground profile location at 1146 feet was concluded to be the hot-spot location used for future ratings analysis. The hot-spot

location can be seen in Figure 9.4. The hot-spot location at 1146 feet on the UG profile corresponds to unscaled DTS data located at 176 m for cable SA.

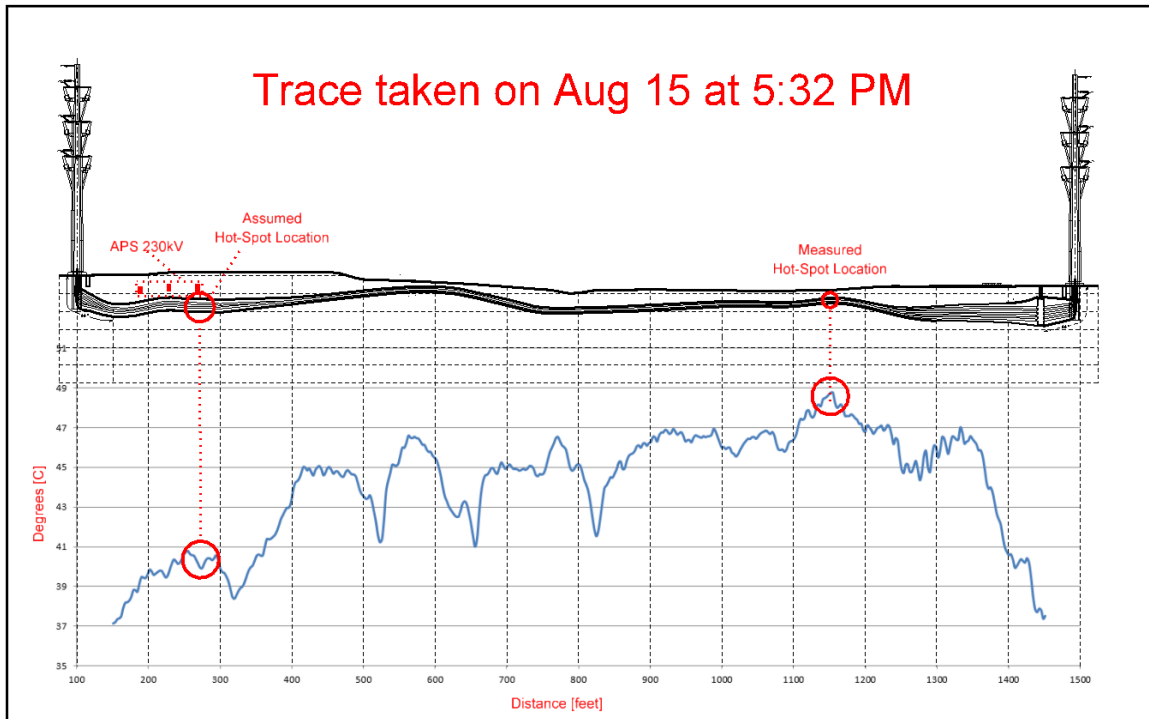


Figure 9.4: DTS Temperature Trace Aligned with UG Profile - Hot-Spot Location Identified

9.2 Measured Temperature at Hot-Spot Location

Continual data collection for UG cable SA began on April 9th 2015. Figure 9.5 and Figure 9.6, respectively, show measured temperatures at 5 minute intervals and averaged daily temperatures at the hot-spot location for the period April 9 through Oct 24 2015.

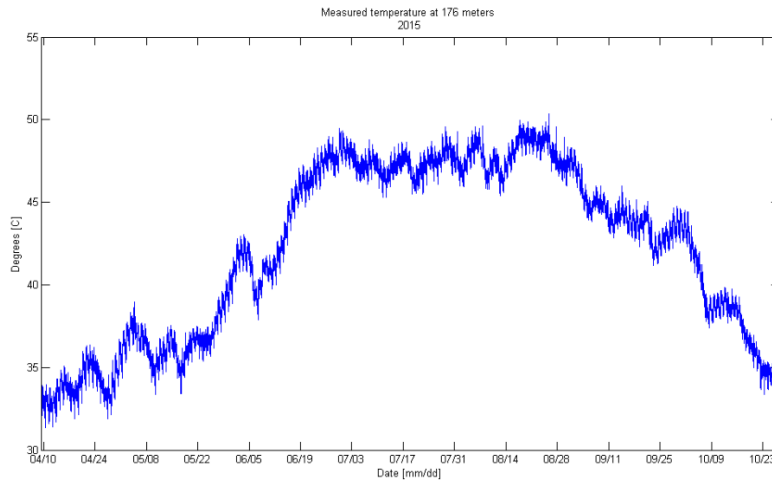


Figure 9.5: Raw DTS Temperature Data at the Hot-Spot Location

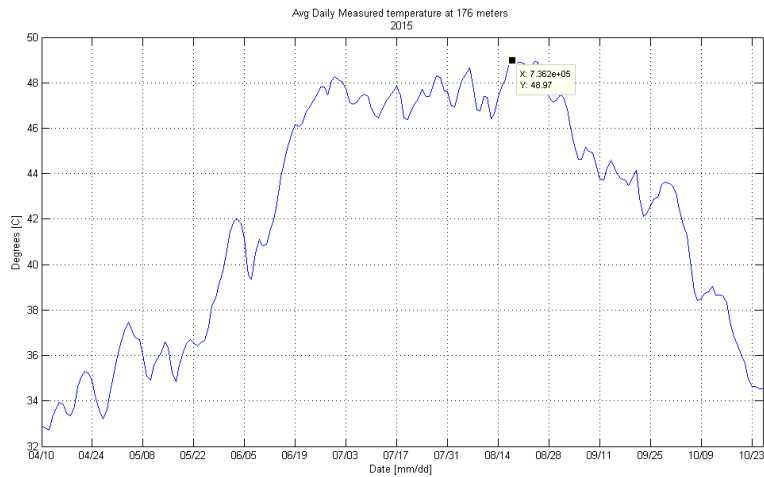


Figure 9.6: DTS Daily Average Temperature at the Hot-Spot Location

The peak measured temperature for the hot-spot location was 50.4 °C and the highest daily average was 48.97 °C. Both occurred on August 18th 2015.

9.3 Evaluation of Steady-State Ampacity at Hot-Spot Location

The original duct bank construction data from the hot-spot location identified in section 9.1 was used to construct a Cymcap model and the steady-state ampacity determined for this location. The original duct bank construction used at the hot-spot location can be found in Figure 4.8. The Cymcap representation can be seen in Figure 9.7 where the bottom layer represents the duct-bank containing the 6 Nexans UG cables (single cable per conduit), the middle layer represents the reinforced concrete that was used at this section and the black upper layer represents the asphalt surface. The surrounding (white) area represents native soil. More details on the duct-bank construction and configuration can be found in section 4.2 and the Cymcap input data used for steady-state Ampacity calculation can be found in Table 9.1.

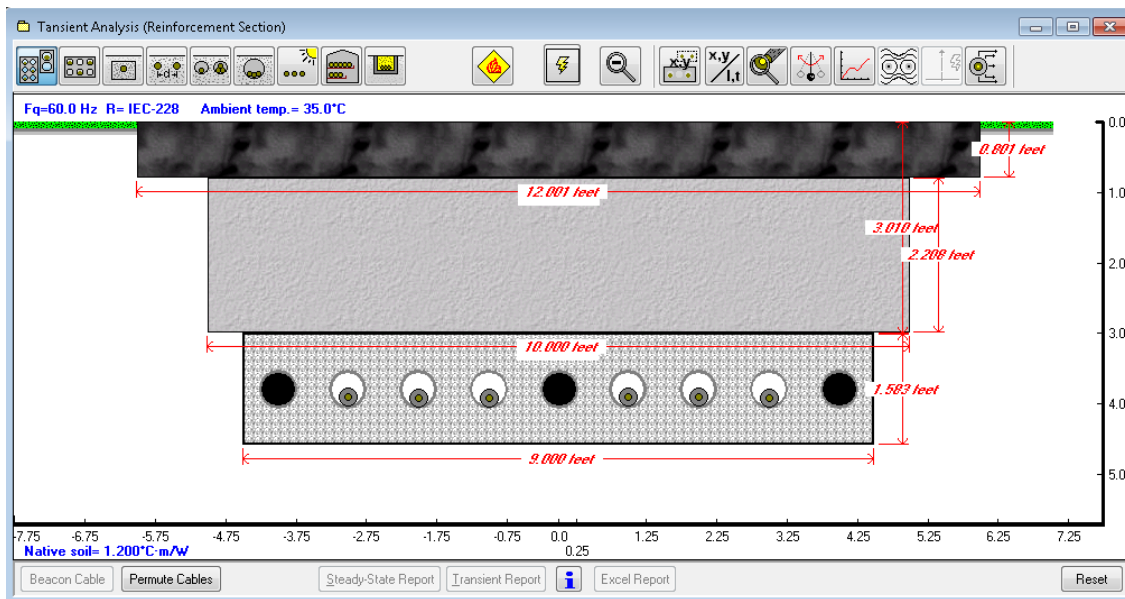


Figure 9.7: Cymcap Duct Bank Model at Hot-Spot Location

Table 9.1: Cymcap Model Input Data

Conductor Temperature	Load Factor	Thermal Resistivity of Native Soil	Thermal Resistivity of Concrete	Thermal Resistivity of Asphalt	Ambient Temperature
90 °C	0.75	1.2 °CmW ⁻¹	1 °CmW ⁻¹	1.3 °CmW ⁻¹	35 °C

The Cymcap model was used to calculate steady-state circuit ampacity using the same ambient temperature (35 °C) as was used in the calculation of the existing ampacity for the Brandow-Pickrell UG circuit. For steady-state ampacity calculation Cymcap determines the maximum continuous current that the cable circuit can carry with no cable conductor exceeding the assigned maximum operating temperature. More detailed explanation of steady-state ampacity calculation can be found in section 2.3. Thermal resistivity values were found using literature sources and assigned to the reinforced concrete and asphalt sections [10]. The Cymcap ampacity calculation yielded a steady-state circuit ampacity of approximately 1800 A at the new hot-spot location. This was 200 A greater than the historic ampacity calculation calculated at the previously assumed hot-spot location described in section 4.4 [3]. This result is expected since the surface ambient temperature was kept the same as was used in the historic ampacity calculation but the distance to the surface was reduced and the thermal resistivities of the reinforced concrete and asphalt were less than the resistivities of the surrounding materials at the assumed hot-spot location used in the historic calculation. The results of the Cymcap modeling suggested that the hot-spot location (according to the current model) should have lower temperatures and not higher than the historical hot-spot. It was suspected that solar irradiation on the asphalt surface was contributing to the higher temperatures of the new hot-spot location.

9.4 Comparison of Cymcap Transient Results to Measured DTS Data

The Cymcap model shown in Figure 9.7 was used to simulate transient cable sheath temperatures at the hot-spot location. Cymcap is capable of performing transient analysis over a maximum of a one week period per simulation. The week of August 19th to the 25th was selected for analysis due to the high ambient temperatures and line loading during this period while maintaining a relatively flat measured temperature profile. Cymcap is capable of using imported transient line loading data as input for transient temperature analysis but uses a fixed ambient temperature for calculation over the 7 day period. Clearly, this is not the desired assumption but it is the state of the art for this software package. For each 7 day period analyzed, the average temperature was found by summing the all of the ambient temperature data samples, $T(k)$, from $k=1, n$, and dividing the total by the total number of measurements. The calculation of average ambient temperature is shown in (9.1) where n is the number of temperature data points. Ambient temperature data was collected from a nearby SRP weather station which recorded temperature measurements every 15 minutes.

$$T_{avg} = \frac{1}{n} \sum_{k=1}^n T(k) \quad (9.1)$$

This average temperature was used as the ambient temperature input into Cymcap for transient analysis. The average ambient temperature for the period of 08/19/2015 to 08/25/2015 was approximately 35 °C and is included in Table 9.2.

The initial conditions for the specified transient analysis period are determined by steady-state analysis which Cymcap performs prior to each transient simulation. In order to most closely match the initial thermal conditions prior to the transient analysis period,

the input current for the steady-state analysis is set to the average line current of the three days prior to the start of the transient analysis period. The average current is computed by summing the line current data samples taken every 15 minutes for the previous 3 days and dividing the total by the total number of measurements. Table 9.2 shows the steady-state current input to Cymcap and the analysis period.

The amplitude of the transient load shape, which is created by Cymcap from the transient input data file supplied by the user, is in per-unit format (each data point of the imported load shape is divided by the maximum value contained in the data set) and thus needs to be scaled appropriately in order to reflect actual line currents. The scaling value is determined by dividing the peak line current (per conductor) for the transient period by the average of previous three-day's currents that is used as input for the steady-state analysis. This is because when Cymcap begins transient analysis, the steady-state current value used for the steady-state initial conditions solution is multiplied by the assigned scaling factor and then by each data point of the per-unit transient load shape in order to scale the load shape back to actual line loading values in ampere. The line loading curve (amperes) in Figure 9.8 is the circuit (two conductors per phase) current for the measurement period shown in Table 9.2 and has a peak of 609 A. For input into Cymcap each data point of the loading curve was divided by two to represent the current for a single conductor. From this halved load shape, Cymcap then creates a load shape with step changes every one hour. This means that four data points from the 15 minute measured line loading data are averaged together for each hour of the resulting Cymcap load shape. It can be seen that multiplying together the scaling factor and the steady-state current of Table 9.2 give one-half (the current per cable) of the peak current value of the

Cymcap load shape seen in Figure 9.9. Table 9.2 lists the relevant Cymcap input data and the DTS measurement location used to produce the measured and calculated temperature data presented in this section.

Table 9.2: Cymcap Transient Analysis Parameters

Measured Cable	DTS Location [m]	Start Date	End Date	Cymcap Scaling Factor	SS Current [A]	Ambient Temperature
SA	176	08/19/2015	08/25/2015	1.264	240	35

Figure 9.8 shows the measured line loading data and measured DTS data related to Table 9.2 and the Cymcap load shape and predicted temperature for the same period can be seen in Figure 9.9.

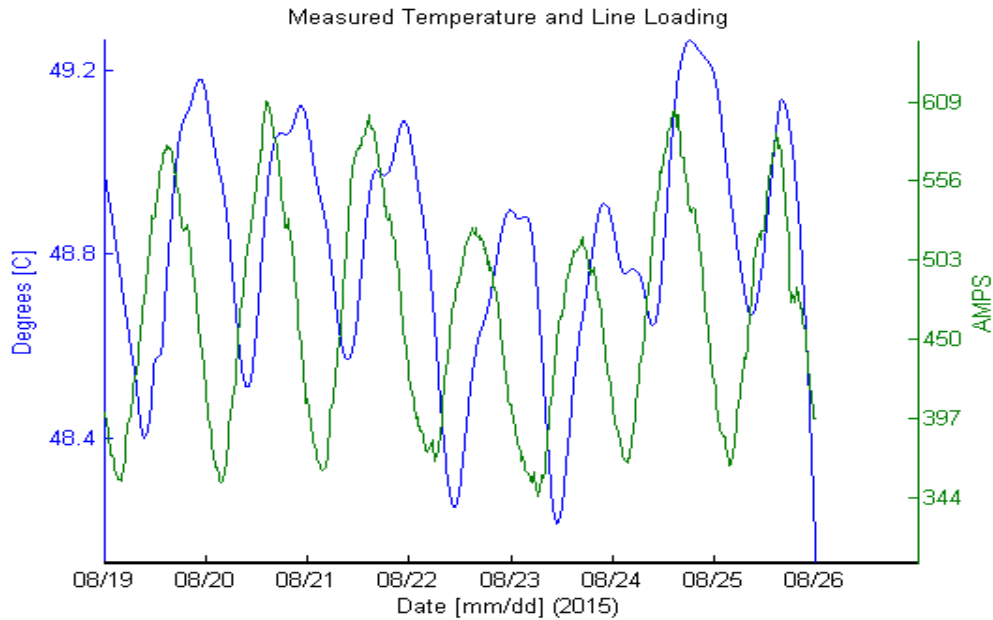


Figure 9.8: Smoothed DTS Temperature Data and Line Loading

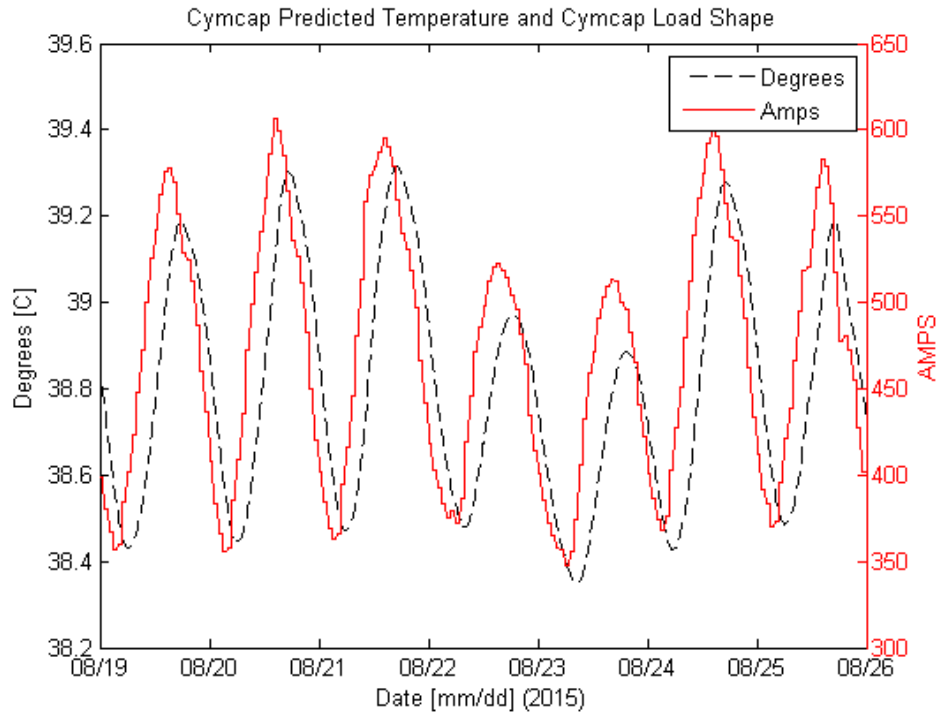


Figure 9.9: Cymcap Load Shape and Predicted Temperature

Since the temperature accuracy of the DTS unit is 1 degree Celsius and the measured temperature profile varied less than this over the 7 day period analyzed, the data shown in Figure 9.8 was processed using Robust Logically Weighted Scatter Plot Smooth (RLOESS) logical regression method. A built in RLOESS smoothing function of Matlab® was used to perform the logical regression smoothing. A detailed description of the process of logical regression can be found in reference source [11]. This helped to reduce signal noise generated by measurement inaccuracies and allowed for better visualization of the measured results. The load shape input into Cymcap and the resulting transient temperature data are displayed in Figure 9.9.

In Figure 9.10 both the DTS measured temperature and the Cymcap predicted temperature (detailed in Table 9.2) are plotted together for comparison.

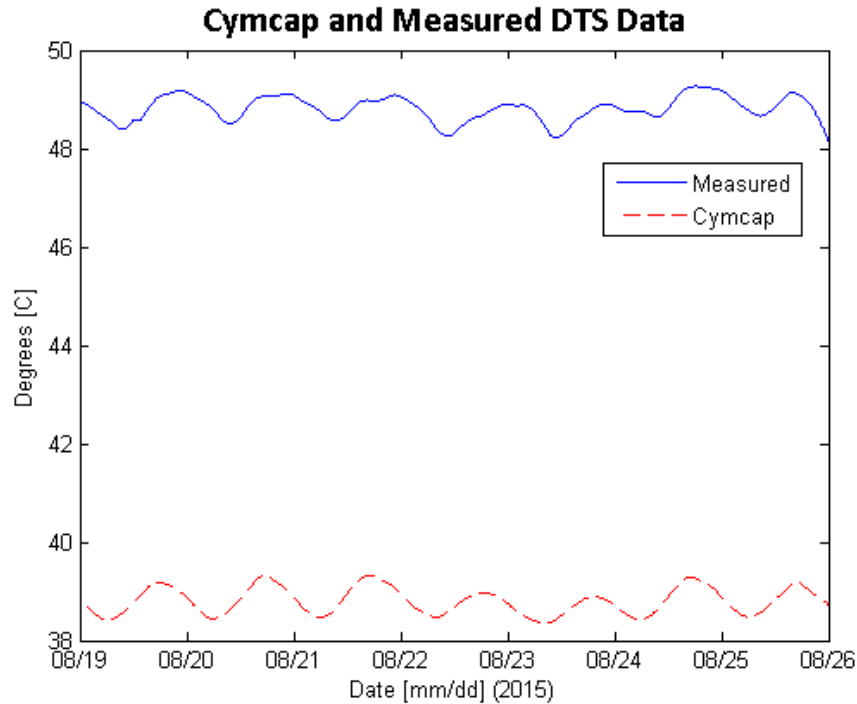


Figure 9.10: Measured DTS and Predicted Cymcap Temperatures with Cymcap Ambient Temperature at 35C

A simple visual inspection of Figure 9.10 shows that the average predicted temperature by Cymcap is approximately 10 °C lower than that of the measured DTS data for the same period. The average temperature for the DTS data was computed according to (9.1) using Matlab and found to be approximately 48.8 °C and the average of the Cymcap data using the same method was found to be approximately 38.8 °C making the shift in average temperature approximately 10 °C.

While the measured and predicted temperatures differed by approximately 10 °C, it should be noted that, for both data sets, the difference between the maximum and minimum hot-spot temperatures for each day as well as the hot-spot temperature behavior (shape) were very similar over the 7 day period. In fact, the difference between the

minimum and maximum temperatures over the measurement period for the DTS data was 1.13 °C and for the Cymcap data was 0.97 °C.

By increasing the ambient temperature setting in Cymcap by 10 °C (from 35 to 45 °C) the transient temperatures predicted much more closely followed the measured temperatures of the DTS. Figure 9.11 shows the Cymcap predicted temperatures with this adjusted ambient temperature compared with the same DTS temperature data presented in Figure 9.10. The average temperature of the adjusted Cymcap result was 48.86 °C which was only 0.06 °C higher than the measured DTS average temperature.

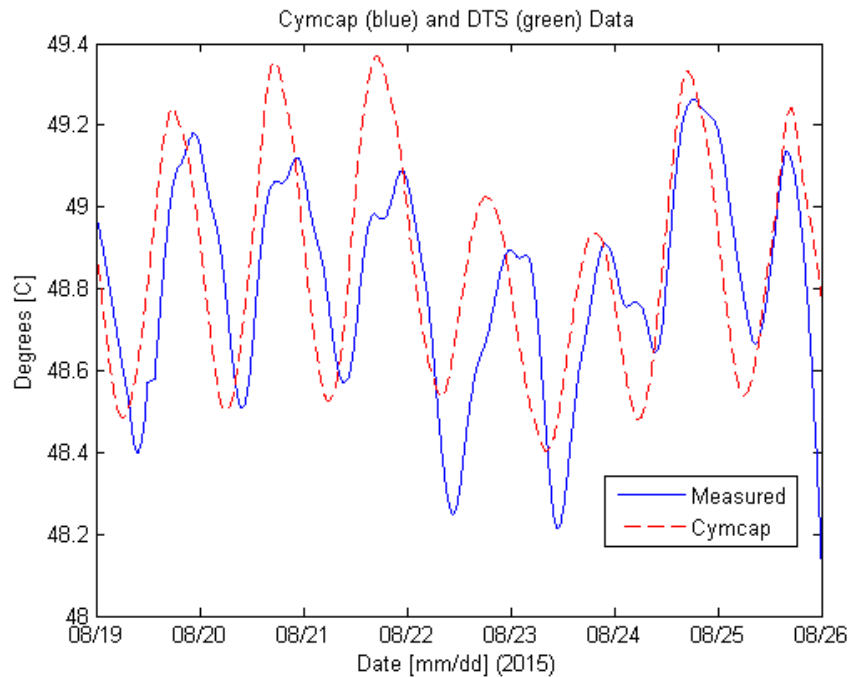


Figure 9.11: Measured DTS and Adjusted Cymcap Temperatures

The large difference between the measured and predicted temperature curves shows that using the daily average of the ambient temperature for calculating cable temperature to be insufficient and inaccurate since it does not consider surface heading due to

solar irradiation. While inaccuracies in the thermal resistivities of the surrounding environment could also be cause for the discrepancy between measured and predicted temperatures that likelihood is much less since much is known from published sources about the thermal resistivities of the commonly used materials that make up the installation. The Cymcap model does not account for surface heating due to solar irradiation and thus this heat source is considered the greatest source of error in the thermal model.

9.5 Adjustment of Ambient Temperature

The 10 °C shift between the averages of DTS measured and Cymcap predicted temperature data for the 7 day period discussed in section 9.4 was thought to be attributed to the asphalt heating on the road surface above the hot-spot location. On August 19th at 2:00 pm an infrared camera was used to survey the road surface directly above the hot-spot location. The maximum temperature detected was 161 °F or 71.7 °C. Figure 9.12 shows the infrared camera display screen while taking a temperature reading from the road surface above the hot-spot location.

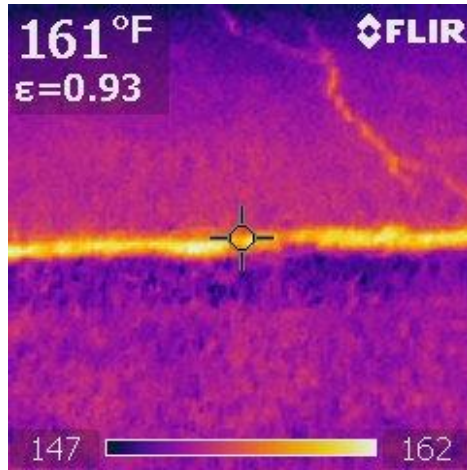


Figure 9.12: Asphalt Temperature above Hot-Spot Location

These hottest measurements only existed along the tar-filled cracks in the asphalt surface. Of the 11 temperature readings taken along the hot-spot surface area, the average reading was 150 °F or 65.6 °C. For comparison, the ambient temperature at the time the asphalt temperatures were read (Aug. 19th 2:00 pm) was 103°F or 39.4°C making the average asphalt temperature reading 26.2 °C higher than the current ambient temperature.

The analysis conducted in Section 9.4 showed that increasing the ambient temperature used by Cymcap for transient temperature analysis resulted in a proportional increase to the average predicted temperature. Using the same assumptions as in section 9.4, one week per month starting in April and ending in October was simulated using Cymcap transient analysis and then compared to recorded DTS data for the same time period. In Table 9.3 each row represents a different 7 day period simulated using Cymcap transient analysis. The average temperature of the resulting Cymcap transient analysis for the cable sheath for each period is listed in column 2. Column 3 shows the average of the recorded DTS temperature data over the same period. The average ambient temperature

listed in column 4, is the average ambient temperature for each period and was used as the ambient temperature setting in Cymcap. Column 5 (Delta) is the required increase for the Cymcap ambient temperature setting which resulted in the averages of both the measured DTS and predicted Cymcap temperatures to converge within ± 0.5 °C. The adjusted ambient temperature shown in column 6 is the addition of column 5 (Delta) to the average ambient temperature of column 4. All average temperatures were calculated according to (9.1) described in section 9.4.

Table 9.3: Cymcap Transient Analysis Results and Required Ambient Temperature Adjustment

Start Date	Cymcap Average Temperature [C]	DTS Average Temperature [C]	Average Ambient Temperature [C]	Delta [C]	Adjusted Ambient Temperature [C]
04/10/2015	24.0	33.3	22.2	9.3	31.5
05/22/2015	24.5	37.2	22.4	12.7	35.1
06/18/2015	40.3	46.5	36.6	6.2	42.8
07/16/2015	36.7	47.1	33.2	10.4	43.6
08/19/2015	38.8	48.8	35.0	10.0	45.0
09/17/2015	32.8	43.4	29.7	10.6	40.3
10/20/2015	24.1	35	22.6	10.9	33.5

While it was expected that the temperature shift (Delta) value would vary more with changes in season, due to varying levels of solar irradiation on the asphalt surface, a relatively constant shift was calculated for each analyzed period. Taking the average of the Delta values of Table 9.3 yielded an average temperature shift of 10.0 °C.

9.6 Re-Evaluation of Steady-State Ampacity with Adjusted Ambient Temperature

Due to the inadequacy of using the average daily temperature when calculating ampacity at the hot-spot location, a reevaluation of the steady-state ratings was conducted using the temperature shift value (Delta) found in section 9.5.

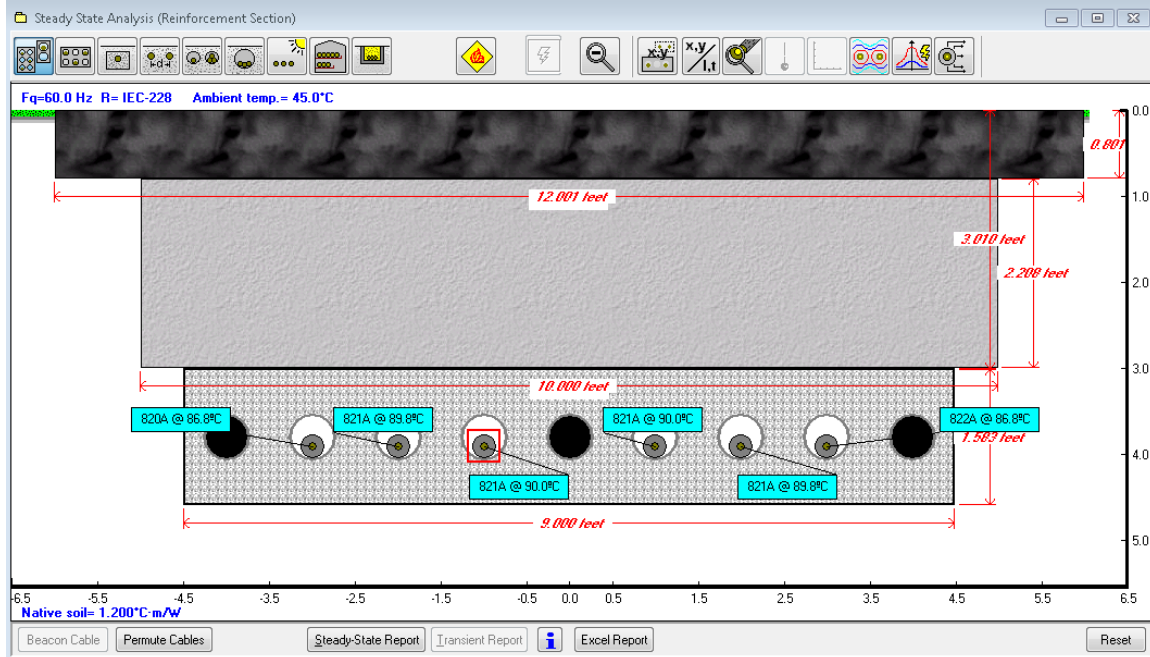


Figure 9.13: Cymcap Reevaluated Steady-State Ampacity

Figure 9.13 shows the Cymcap steady-state ampacity calculation results using the adjusted ambient temperature value of 45 °C. The reevaluated steady-state circuit ampacity was found to be 1640 A. This is 160 A less than the ampacity result found using the standard ambient temperature value of 35 °C which was used in the earlier evaluation of section 9.3.

10. SUMMARY, CONCLUSIONS AND FUTURE WORK

10.1 Distributed Temperature Sensing (DTS)

The DTS used in this work was designed for use with 50/125 micron multi-mode optical fibers. It was learned during preliminary research on the then proposed Brandow-Pickrell UG monitoring site that a mix of both 50/125 and 62.5/125 micron multi-mode fibers had been used. The DTS manufacturer could not definitively state whether their unit would perform to its rated specifications given that mixed fiber diameters would be used. A small-scale controlled testing setup was constructed to simulate the fiber configuration at the Brandow-Pickrell UG installation. By using a dual-ended loop measurement configuration it was determined that the DTS could measure fiber temperatures within the manufacturers stated accuracy. The detailed analysis is presented in Chapter 5.

10.2 Hot-Spot Locating

For underground transmission lines installed without the ability to directly measure cable temperatures the deepest portion is often used as the cable hot-spot location. For an installation of uniform backfill, duct bank, burial depths which do not come into “close” proximity with the surface and native soil properties and without the presence of any heat sources this assumption will hold true. Most underground power cables however, are installed in residential and city areas making the underground path shared with the infrastructure of other utilities and have more complex underground environments that change along the installation path. Note that Cymcap ampacity calculation standards consider a distance as “close” to the earth surface (and do not guarantee accurate results)

when the ratio $d/L_e < 0.4$ or cable depths of less than 1.5 m. L_e (meters) is the distance from the earth surface to the closest conductor and d (meters) is equal to $1/ar_0$ where a ($\text{W}\cdot\text{m}^{-2}\cdot^\circ\text{C}^{-1}$) is the convection coefficient of the air earth interface and r_0 ($^\circ\text{C}\cdot\text{m}\cdot\text{W}^{-1}$) is the thermal resistivity of the native soil.

DTS was used to take temperature traces of the SRP controlled Brandow-Pickrell 69 kV underground circuit. Temperature trace data was taken every 5 minutes over a period 6 months. The collected data was analyzed and used to locate the true hot-spot of the UG cable. It was shown that the true hot-spot location for the Brandow-Pickrell line was not at the assumed, deepest, section but instead at one of the shallowest portions which came into close proximity with the asphalt road surface above. Asphalt temperature readings were taken that indicate asphalt surface heating (due to solar irradiation) was likely the main contributor to the hot-spot location being at this shallower location. Using the SRP provided underground profile of the installation as reference, the measured hot-spot location was located at position 1146 feet. The underground profile showing the hot-spot location and the locating analysis can be seen in section 9.1.

The hot-spot locating analysis showed that the commonly made assumption that the deepest portion of an underground power cable installation will be the hot-spot does not always hold true. The results showed that performing distributed cable temperature measurements for UG power cables could be used to locate the proper segment to be used for ampacity calculations.

10.3 Ampacity Calculation at new Hot-Spot Location

The new hot-spot location was modeled using Cymcap cable ampacity software. Steady-state ampacity was found using the same ambient temperature value of 35 °C that was used for the calculation of the historic circuit ampacity of 1600 A. Using this ambient temperature value, Cymcap calculated a steady-state circuit ampacity of 1800 A. A detailed description of the ampacity calculation can be found in section 9.3.

10.4 Ambient Temperature Adjustment

To evaluate the accuracy of the rating, Cymcap transient analysis was performed using measured line loading data as input. Transient cable temperature for a 7 day period was calculated. The ambient temperature used in the Cymcap calculation was the average temperature of the 7 day period. This produced a transient temperature curve with an offset of 10 °C. This is consistent with the average surface temperature being elevated due to solar irradiation on the asphalt surface above the hot-spot location. Further analysis on the asphalt heating was performed by evaluating the required increase to ambient temperature used in the Cymcap transient calculation for different 7 day periods during each month data was collected. A total of 7 weeks were evaluated spanning nearly 7 months. It was concluded that an average temperature increase to ambient of 10 °C was required for the Cymcap average temperature to align with the average DTS measured temperature of the same period. This result indicated that if an ambient temperature of 45 °C is used for steady-state ampacity calculations for this site, rather than the typical value of 35 °C, the steady-state ampacity simulation results are likely to be more accurate.

10.5 Reevaluation of Steady-State Ampacity at Hot-Spot Location

Using the adjusted ambient temperature of 45 °C the Cymcap hot-spot location model was used to calculate steady-state circuit ampacity. The ampacity using the adjusted ambient temperature found was 1640 A which was a decrease in rating of 160 A from the first simulation.

10.6 Proposed Future Work

10.6.1 Surface Temperature Measurement and Effective Thermal Resistivity Estimation

The thermal resistivities of the concrete duct bank and the asphalt surface at the measured hot-spot location were estimated using literature values. Also the exact depth of the duct bank at the measured location was not recorded at the time of installation and had to be estimated as well. Using DTS along with accurate ambient and surface temperature readings at the measurement site, the effective thermal resistivity from the cable conductor to the surface can be calculated [12]. Accurate measurements of the temperature profile at the hot-spot location surface can also be used to determine the accuracy of the Cymcap model given the shallow depth limitation discussed in section 10.2.

10.6.2 Dynamic Thermal Ratings

If appropriate measurement devices were installed at the hot-spot surface, future work could allow for the construction and implementation of a process to evaluate and estimate the effective thermal resistivities for underground cable installations. With the accurate thermal properties, a system of dynamic thermal ratings could be developed which would allow for greater utilization of installed underground transmission assets for electric utilities.

REFERENCES

- [1] T. Wang, "Thermal Performance of 69kV Underground Cables," Arizona State University, Tempe, 2013.
- [2] Nexans, "60-500 kV High Voltage Underground Power Cables," Paris, France, 2011
- [3] SRP, "SRP 69kV Underground Installed Projects," 2012.
- [4] J. H. N. a. M. H. McGrath, "The calculation of the temperature rise and load capability of cable systems," *AIEE Transactions* , vol. 76, pp. 752-772, 1957.
- [5] W. r. Humbert, "Measurement of the permittivity and loss tangent of dielectric sheets," *Microwave and Optical Technology Letters*, vol. 15, no. 6, 1997.
- [6] C. International, "cyme," COOPER Power Systems, [Online]. Available: <http://www.cyme.com/software/cymcap/BR917028EN-CYMCAAP.pdf>. [Accessed 09 10 2014].
- [7] EPRI, "EPRI Underground Transmission Systems Reference Book," EPRI, 2007.
- [8] IEC, "IEC. (2006). IEC Electric cables - Calculation of the current rating".
- [9] N. v. d. Giesen, "Double-Ended Calibration of Fiber-Optic Raman Spectra Distributed Temperature Sensing Data," no. 12, pp. 5471-5485, 2012.
- [10] J. I. Adams, "The Thermal Behavior of Cable Backfill Materials," *Power Apparatus and Systems*, vol. 87, no. 4, pp. 1149-1161, 2007.
- [11] G. Rodriguez, "Smoothing and Non-Parametric Regression," Princeton University, Princeton, NJ, 2001.
- [12] K. C. T. a. Q. S. H. J. Li, "Assessment of Underground Cable Ratings Based on Distributed Temperature Sensing," *IEEE Transactions On Power Delivery*, vol. 21, no. 4, pp. 1763-1769, 2006.
- [13] K. L. Hall, "Out of Sight, Out of Mind," Edison Electric Institute, Washington, D.C., 2012.
- [14] G. Anders, Rating of Electric Power Cables in Unfavorable Thermal Environment, Hoboken, N.J.: Wiley, 2005.
- [15] "IEEE Standard Power Cable Ampacity Tables, IEEE Std. 835-1994".

[16] NEMA, "NEMA Enclosure Types," National Electrical Manufacturers Association, Rosslyn, VA, 2005.